

The Design of a Martian Lander for Crew and Cargo

a project presented to
The Faculty of the Department of Aerospace Engineering
San José State University

in partial fulfillment of the requirements for the degree
Master of Science in Aerospace Engineering

by

Alec B. Gloria

December 2021

approved by

Dr. Periklis Papadopoulos
Faculty Advisor



San José State
UNIVERSITY

© 2021
Alec B. Gloria
ALL RIGHTS RESERVED

ABSTRACT

The Design of a Martian Lander for Crew and Cargo

Alec B. Gloria

This report details the design of a Martian landing system for transporting crew and cargo from Martian orbit to the Martian surface. A literature review was conducted that determined liquid methane and oxygen are effective propellants. Furthermore, a staged approach to a landing system is feasible for a mission to Mars. A system level design is created with the following subsystems:

- Propulsion
- Life Support
- Thermal
- GNC
- Structures

An engine design is developed for the propulsion subsystem with a specific impulse of 248 seconds and a thrust of 2.42 MN (0.544×10^6 lbf). This engine is simulated and analyzed in varying atmospheric pressures and the engine design is shown to meet mission needs. Historical orbital trajectory data from successful Mars missions is compiled and analyzed. Orbital dynamic theories were reviewed and inputs were calculated for GMAT simulations. The simulations provided the most effective interplanetary transfer: a semi-direct interplanetary Hohmann transfer. Theoretical and simulated trajectories show:

- A delta-V requirement of 2.94 km/s (9.65×10^3 ft/s)
- A transit period of approximately 258.8 days,
- A total mission duration being a minimum of 2.7 years.

Program development and mission logistics analysis show an 11-year development cycle and testing program is feasible for creating the Martian Landing System.

ACKNOWLEDGEMENTS

I would like to thank the healthcare worker community, victims of social injustice and their advocates, the CalFire community, the men and women of the National Guard who defended democracy at home, and the men and women of the Armed Forces who gave life or limb defending democracy abroad; all of whom served as an incredible and never-ending source of inspiration during these unprecedented and difficult times.

I would also like to thank my friends and family for their continuous support, patience, and understanding as I receded from countless obligations to focus on my career and education. A special thank you to my advisor, Dr. Papadopoulos, for his guidance on this project. I would also like to thank the other kind and helpful staff/faculty of the Aerospace Department as well as my fellow peers who helped along the way.

TABLE OF CONTENTS

ABSTRACT	iii
ACKNOWLEDGEMENTS	iv
TABLE OF CONTENTS	v
LIST OF TABLES	vii
LIST OF FIGURES	viii
SYMBOLS	x
Chapter 1: Introduction, Literature Review, and Methodology	1
1.1 Literature Review.....	2
1.1.1 Human Landing Systems	2
1.1.2 Propulsion Applications for Mars	4
1.1.3 Orbital Dynamics	5
1.1.4 Mission Logistics	7
1.2 Literature Review Conclusions.....	8
1.3 Project Objective.....	9
1.4 Methodology	9
Chapter 2: System Level Design of a Martian Lander for Crew and Cargo	11
2.1 Preliminary Estimate of Mission Requirements and Constraints	11
2.1.1 Historical Data	11
2.1.2 Current and Future Launcher Capabilities	12
2.1.3 Requirement and Constraint Analysis	12
2.2 Characterizing Mission Architecture and Concepts	13
2.2.1 Concept of Operations	13
2.2.2 Subsystem Overview	14
2.2.3 Propulsion	14
2.2.4 Life Support	14
2.2.5 Thermal.....	14
2.2.7 Guidance, Navigation, and Control	15
2.2.8 Structures	15
2.3 N2 Diagram and Requirements.....	15
2.3.1 N2 Diagram.....	15
2.3.2 Requirements	17
Chapter 3: Propulsion Subsystem Design	19
3.1 Historical Data and Analysis	19
3.2 Nozzle Design.....	20

3.3 CFD Analysis.....	26
3.3.1 Geometry.....	26
3.3.2 Meshing.....	26
3.3.3 Simulations	28
3.4 Propulsion Subsystem Conclusions	35
Chapter 4: Orbital Dynamics	37
4.1 Historical Data and Analysis	37
4.2 Theory.....	38
4.3 Simulation.....	42
4.4 Conclusions.....	47
Chapter 5: Program and Mission Planning	48
5.1 Project Development.....	48
5.1.1 Earth-based Testing Milestones.....	48
5.1.2 Low-Earth Orbit-Based Testing Milestones	50
5.1.3 Mars-Based Testing Milestones.....	50
5.1.4 Production Line Qualification Milestones	51
5.1.5 Schedule.....	51
5.2 Module Descriptions and Concept of Operations.....	53
5.3 Mission Operations	56
5.4 Program Benefits	57
References.....	58
Appendix A – Sample Hand Calculations	60

LIST OF TABLES

Table 2.1 - Comparison of historical lander data.....	11
Table 2.2 - Launcher comparison	12
Table 2.3 - Preliminary MLS requirements	17
Table 3.1 - Historical propulsion data.....	19
Table 3.2 - Engine design parameters.....	20
Table 3.3 - Propulsion parameters	23
Table 3.4 - Quality metric summary	28
Table 4.1 - Historical mars mission data	37
Table 4.2 - Trajectory types between Earth and Mars	39
Table 4.3 - Launch opportunities	40
Table 4.4 - Mission durations	42
Table 5.1 - Earth-based milestones.....	49
Table 5.2 - Low earth orbit milestones	50
Table 5.3 - Mars based testing milestones	51
Table 5.4 - Production line milestones	51
Table 5.5 - MLS program schedule	52

LIST OF FIGURES

Figure 2.1 - N2 diagram.....	16
Figure 3.1 - Specific heat ratio plot	21
Figure 3.2 - Minimum nozzle length verification plot.....	22
Figure 3.3 - Specific impulse verification plot	22
Figure 3.4 - Thrust verification plot.....	23
Figure 3.5 - Intersection point diagram.....	25
Figure 3.6 - Characteristic lines	25
Figure 3.7 - Nozzle geometry	26
Figure 3.8 - Simulation geometry	26
Figure 3.9 - Mesh.....	27
Figure 3.10 - Nozzle mesh	27
Figure 3.11 - Skewness metrics	27
Figure 3.12 - Orthogonality metrics.....	28
Figure 3.13 - Pressure contour for $P_0 = 101,325$ Pa.....	28
Figure 3.14 - Mach number contour for $P_0 = 101,325$ Pa	29
Figure 3.15 - Residuals for $P_0 = 101,325$ Pa	29
Figure 3.16 - Pressure contour for $P_0 = 80,000$ Pa.....	29
Figure 3.17 - Mach number contour for $P_0 = 80,000$ Pa	30
Figure 3.18 - Residuals for $P_0 = 80,000$ Pa	30
Figure 3.19 - Pressure contour for $P_0 = 60,000$ Pa.....	30
Figure 3.20 - Mach number contour for $P_0 = 60,000$ Pa	31
Figure 3.21 - Residuals for $P_0 = 60,000$ Pa	31
Figure 3.22 - Pressure contour for $P_0 = 40,000$ Pa.....	31
Figure 3.23 - Mach number contour for $P_0 = 40,000$ Pa	32
Figure 3.24 - Residuals for $P_0 = 40,000$ Pa	32
Figure 3.25 - Pressure contour for $P_0 = 20,000$ Pa.....	32
Figure 3.26 - Mach number contour for $P_0 = 20,000$ Pa	33
Figure 3.27 - Residuals for $P_0 = 20,000$ Pa	33
Figure 3.28 - Pressure contour for $P_0 = 10,000$ Pa.....	33
Figure 3.29 - Mach number contour for $P_0 = 10,000$ Pa	34
Figure 3.30 - Residuals for $P_0 = 10,000$ Pa	34
Figure 3.31 - Pressure contour for $P_0 = 6,000$ Pa.....	34
Figure 3.32 - Mach number contour for $P_0 = 6,000$ Pa	35
Figure 3.33 - Residuals for $P_0 = 6,000$ Pa	35
Figure 4.2 - Hohmann transfer diagram.....	40
Figure 4.3 - Earth departure	42
Figure 4.4 - Earth departure closeup.....	43
Figure 4.5 - Hohmann transfer trajectory	43
Figure 4.6 - Hohmann transfer isometric view	44
Figure 4.7 - Mars orbit insertion.....	44
Figure 4.8 - Mars orbit insertion closeup.....	45
Figure 4.9 - Mars orbit departure.....	46
Figure 4.10 - Mars to earth orbital trajectory.....	46
Figure 4.11 - Earth arrival.....	47

Figure 5.1 - Crew module	53
Figure 5.2 - Cargo module	54
Figure 5.3 - Descent module with crew module	54
Figure 5.4 - Descent module with folded heat shield to return to orbit	55
Figure 5.5 - Descent module with cargo module and fuel module	55
Figure 5.6 - Descent module with crew module in transit configuration	56

SYMBOLS

Symbol	Definition	Units (SI)
A^*	Critical Diameter	ft (m)
A_e	Nozzle Exit Diameter	ft (m)
C-	Right Running Characteristic Angle	deg
C+	Left Running Characteristic Angle	deg
F	Thrust	lbf (N)
g_0	Earth Gravity	ft/s ² (m/s ²)
I_{sp}	Specific Impulse	sec
K-	Right Running Characteristic Constant	
K+	Left Running Characteristic Constant	
L_N	Length of Nozzle	ft (m)
M	Mach Number	
M_e	Exit Mach Number	
\dot{m}	Mass Flow Rate	lbm/s (kg/s)
n	Periodic Multiplication Variable	
O/F	Oxidizer to Fuel Ratio	
P_e	Nozzle Exit Pressure	PSI (Pa)
P_t	Nozzle Throat Pressure	PSI (Pa)
R	Ideal Gas Constant	
R_{EARTH}	Earth Orbital Radius	ft (m)
R_{MARS}	Mars Orbital Radius	ft (m)
T	Temperature	R (K)
T_e	Nozzle Exit Temperature	R (K)
$T_{HISTORICAL}$	Historical Launch Date	
$T_{SURFACE}$	Surface Mission Duration	day
$T_{SYNODIC}$	Synodic Period Between Earth and Mars	day
$T_{TRANSIT}$	Travel Time Period Between Earth and Mars	day
T_{LAUNCH}	Launch Date	
T_t	Nozzle Throat Temperature	
v_e	Exit Velocity	ft/s (m/s)
γ	Specific Heat Ratio of Mixed Propellant	
γ_{gas}	Specific Heat Ratio of Specified Gas	
$\gamma_{methane}$	Specific Heat Ratio of Methane	

Symbol	Definition	Units (SI)
γ_{oxygen}	Specific Heat Ratio of Oxygen	
γ_{perf}	Ideal Gas Specific Heat Ratio	
$\Delta V_{\text{ARRIVAL}}$	Arrival Velocity Change at Mars	ft/s (m/s)
$\Delta V_{\text{DEPARTURE}}$	Departure Velocity Change from Earth	ft/s (m/s)
Θ	Thermal Constant	R (K)
θ	Flow Angle	deg
θ_{max}	Maximum Flow Angle	deg
μ	Mach Angle	deg
μ_{SUN}	Gravitational Parameter of the Sun	ft ³ s ⁻² (m ³ s ⁻²)
ν	Prandtl-Meyer Angle	deg
ADEPT	Adaptive Deployable Entry and Placement Technology	
ARM	Asteroid Redirect Mission	
CFD	Computational Fluid Dynamics	
COTS	Consumer Off the Shelf	
CTB	Cargo Transport Bags	
ECLS	Environmental Control and Life Support	
EDL	Entry, Descent, and Landing	
GMAT	General Mission Analysis Tool	
GNC	Guidance, Navigation, and Control	
HIAD	Hypersonic Inflatable Aerodynamic Decelerator	
HMC	Heat Melt Compactor	
ISS	International Space Station	
KSC	Kennedy Space Center	
LEO	Low-Earth Orbit	
LDAC-4	Lunar Module	
LM	Lunar Module	
LPL	Lunar Pallet Lander	
MAV	Mars Ascent Vehicle	
MLS	Mars Landing System	
MSFC	Marshall Space Flight Center	
RCS	Reaction Control System	
RFID	Radio Frequency Identification	
SLS	Space Launch System	
SSTO	Single-Stage to Orbit	
TCM	Trajectory Correction Maneuver	
TCS	Traditional Control System	

Symbol	Definition	Units (SI)
TLI	Trans-Lunar Injection	
TMI	Trans-Mars Injection	
TRL	Technology Readiness Level	
UWMS	Universal Waste Management System	

Chapter 1: Introduction, Literature Review, and Methodology

Human-rated spacecraft have been conceptualized, designed, and flown multiple times since the beginning of human spaceflight. The longest serving spacecraft today is the International Space Station (ISS). The ISS has been continuously operated and inhabited by a multinational crew for the past 20 years. However, the ISS cannot be operated as an independent spacecraft and requires auxiliary spacecraft to provide transport for crew and cargo. The constant transportation missions from Earth do not pose a large logistical problem because of the location of the space station in Low Earth Orbit. There are also multiple launch providers that provide flight-proven transportation spacecraft.

There is now a technological push to send human-rated spacecraft beyond LEO. NASA's Artemis Program plans to establish a permanent research station in Lunar orbit over the next decade, called Gateway. Gateway will be used as a launching point for Lunar surface missions and the development of a permanent outpost on the surface. Lunar landers are currently being researched and developed to transport crew and cargo between Gateway and the Lunar surface. The Moon will serve as a proving ground to develop and test lander technologies that can also be used on Mars.

Designing a Martian lander is far more complex than it is to design a spacecraft that can land on the Moon or return to Earth. The additional complexities originate from Mars having an atmosphere much less dense than the atmosphere of Earth. Additionally, Mars is much further away than LEO or the Moon. Unlike a Lunar Lander, a Martian lander will need a heat shield to enter the atmosphere. The increased distance from Earth adds the requirement to reduce speed from a greater velocity in a thinner atmosphere. The spacecraft must also operate independently from mission control. These requirements for safely landing crew and cargo on Mars established the need for a Martian lander that is more complex than any of the current or planned transportation spacecraft.

1.1 Literature Review

This section contains summaries of twenty works of literature on the topic of human spacecraft design. Four topics are researched:

- Human Landing Systems
- Propulsion Applications for Mars
- Orbital Dynamics
- Mission Logistics

Sources are of varying types which include:

- NASA Technical Reports
- Industry Journals
- Conference Papers
- Textbooks

1.1.1 Human Landing Systems

The human desire to explore space is best summarized by a quote from Krafft Ehrlicke, “If God wanted man to become a spacefaring species, he would have given man a moon,” [1]. The first lander to take humans to a celestial object, other than Earth, was the Apollo Lunar Module (LM). The LM design is purely functional with the goal to safely land two humans on the surface of the Moon and return them to Lunar orbit. To achieve this goal, the LM is designed to provide living space and utilities for multi-day missions. The LM is also capable of large velocity changes to decelerate from and accelerate to Lunar orbital speeds of 4,473.9 mph [1].

All other lander designs in this report did not advance past the conceptual phase. Since no physical hardware was built for these designs, only two design methods were used: “bottoms-up” and “parametric” design [1]. In bottoms-up design, subject matter experts in various spacecraft subsystems provide subsystems designs. Systems engineers will take this data and provide an estimate of overall vehicle performance. This method only offers a partial picture of vehicle performance. This is due to the highly coupled nature of certain subsystems. This coupling leads to constantly evolving performance characteristics as spacecraft designs progress through development. Therefore, parametric design principles can be used where certain performance characteristics that cannot be immediately determined are estimated based on historical data. For example, the structural subsystem can only provide an estimate for the secondary structures required by the other spacecraft subsystems. Other subsystems such as life-support need to be fully designed to get a better picture of all the bracketry and supports needed for life-support hardware [1]. A combination of bottoms-up and parametric design proves to be a successful method of design as shown by the numerous lander designs that were.

The latest iteration of NASA’s Mars lander also used the design technique discussed in “After LM, NASA Lunar Lander Concepts Beyond Apollo.” The design of a Mars ascent vehicle (MAV) required careful thought and consideration of all subsystem design aspects. The MAV performance has a direct effect on meeting overall mission requirements.

The mass of the MAV determines the following:

- Launch vehicle used on Earth
- The payload that can be transported to and from the surface
- Reentry dynamics
- Mission duration

The MAV in “Mars Ascent Vehicle Design for Human Exploration,” has two stages of equivalent thrust with three engines on the first stage and one engine on the second stage [2]. The MAV lands on the Martian surface without oxidizer, but it is designed to produce its own oxidizer supply from the Martian atmosphere [2]. However, due to the slow nature of oxygen production, the MAV needs to land years in advance before use. Additionally, the MAV needs to be connected to an additional land based power supply after landing [2]. The structure of the MAV is minimal with a crew compartment design similar to a traditional spacecraft. However, fuel and oxidizer tanks are mounted externally without shielding [2]. The MAV has a thermal control system (TCS) as well avionics and environmental control and life support (ECLS) subsystems based on Altair lunar landing system [2]. This report serves as a preliminary study to determine which technologies are needed to develop a MAV, such as fuel production, and heat shield development. A larger and more advanced lander will be needed to successfully land both crew and cargo on Mars. However, this report suggests Multiple smaller MAVs can also successfully support a mission to Mars.

As suggested in other technical reports, a human lander for Mars requires technologies that are far more advanced than what exists today. In “Human Mars Lander design for NASA’s evolvable mars campaign,” advancements in:

- Payload delivery
- Precision landing
- Entry, descent, and landing (EDL)

are necessary to land humans safely and successfully on Mars [3]. Two entry systems that are currently under investigation are the Hypersonic Inflatable Aerodynamic Decelerator (HIAD) and Adaptable Deployable Entry and Placement Technology (ADEPT) [3]. Both conceptual entry system technologies can deploy a heat shield far larger than the fairing diameter of currently existing launchers. This allows for larger payloads to be landed on the surface of Mars. The lander described in this report is configurable to different payloads:

- a MAV
- a single large habitat module
- multiple smaller payloads
- rovers
- secondary modules [3].

Technologies do not yet exist that allow for the landing of all mission hardware at once. As discussed previously, multiple landers are required with each capable of delivering 27 tons to the Martian surface.

The technical report, “Mission design for the lunar pallet lander,” further emphasizes the benefit of having separate lander modules for different function. NASA is developing a Lunar

pallet lander (LPL) to deliver relatively small payloads, up to 300 kg, to the polar surfaces of the Moon [4]. The lander can perform Trajectory Correction Maneuvers (TCMs) for a precise landing [4]. Currently, the LPL is not included in mission planning for the Artemis program, so the LPL is designed with generic cargo in mind. The lunar poles are of great interest to researchers, as there is evidence of water ice in these areas [4]. The also lander includes a decent stage that is ejected before the landing stage ignites its thrusters for a soft landing.

Textbook resources such as “Manned Spacecraft Design Principles,” also support the design principles found in the previously discussed technical reports [5]. To get the most successful design, a combination of parametric and bottoms-up design is needed [5].

1.1.2 Propulsion Applications for Mars

A mission to Mars requires the use of propulsion systems at multiple stages of the mission:

- Launch,
- Transport
- Landing
- Return

Multiple propulsion systems are being investigated for missions to Mars, including hybrid propulsion. Hybrid propulsion consists of a solid fuel and liquid oxidizer. In “Mars Ascent Vehicle Hybrid Propulsion,” hybrid propulsion is investigated for use on a MAV to conduct sample return missions on the Martian surface [6]. Benefits of a hybrid propulsion system include use at low temperatures and a higher Specific Impulse which could allow single stage to orbit (SSTO) capabilities from Mars [6]. The disadvantages are that the Technology Readiness Level (TRL) is lower than that of traditional liquid fueled or solid fueled propulsion systems [6]. The hybrid design allows for a unique construction of the MAV, such that helium pressurization and ignitor fluid tanks can be positioned around the solid rocket motor. Fuel for the reaction control system (RCS) can also be housed in this area [6]. This volume around the solid rocket motor is a result of the fuel-grain regression dynamics which show that the fuel grain diameter can be much smaller than the diameter of the oxidizer tank [6]. The motor itself is a wax-based fuel grain. Unlike traditional solid rocket motors, hybrid motors can be reignited which make it an attractive option for future MAVs.

Electric propulsions systems are compared to nuclear and bi-propellant systems for use in Martian applications in “Manned Mars Landing Missions Using Electric Propulsion,” [7]. The systems are investigated for a seven-person crew over a forty-day Mars exploration mission. This report determines that the most efficient means of electric propulsion is a combination of both electric and nuclear propulsion [7]. A combination with nuclear propulsion is attractive due to the high thrust capabilities a nuclear system provides. Propellants for the electric propulsion system can be Mercury or Cesium [7]. To maximize propellant savings with electric propulsion, long propulsion periods are desired. Atmospheric breaking is also considered in this design to reduce the amount of fuel needed [7]. Atmospheric breaking is a fuel conservation strategy that can be utilized with other propulsion systems as well.

A bi-propellant oxygen and methane system is investigated for use on missions to Mars in “Methane propulsion elements for Mars,” [8]. Methane is advantageous for Martian surface access because it can be produced from the Martian atmosphere. The Methane is useful for Martian landing applications. However, by utilizing methane for all mission vehicles, design complexity can be reduced by introducing commonality between propulsive elements [8]. This also reduces the need to transport Earth-based fuels.

A solid propulsion configuration for a MAV was investigated as a risk mitigation option to the hybrid motor also being researched for the same application. Although a purely solid configuration does not have SSTO or throttling capabilities, it does have a higher TRL and has been flight-proven on other applications [9]. A two-stage solid-fuel design can provide sample return capabilities with a payload of 16 kilograms [9]. This design is currently theoretical as it includes thrust vectoring which is not typically found on solid rocket motors, and it is designed to be operated in the Martian atmosphere [9]. Another unique aspect of this propulsive design is that the solid rocket grains are spherical with a star shaped core to facilitate even regression dynamics. In conjunction with the solid fuel as a primary propellant, the MAV in this report contains a hydrazine reaction control system (RCS) [9].

Textbook sources such as “Liquid Propellant Rocket Engines,” provide a basic overview of propulsion components and the methodology behind designing an engine [10]. The liquid propellant rocket engines chapter in this textbook discusses all the basic components of a liquid propellant rocket. This textbook also discusses the combustion of propellants as well as performance characteristics. Methods for cooling as well as examples of propellant flow are provided in this textbook.

1.1.3 Orbital Dynamics

The orbital dynamics of a crewed mission to Mars need to be carefully analyzed to develop the ideal trajectory in a minimal amount of time. NASA recommends a 180 day mission [11]. However, increasing the mission duration to 270 days reduces the required delta V by up to 50% in “Trajectories for Human Missions to Mars, Part 1: Impulsive Transfers [11]. A key reason for optimizing orbital trajectories is the deteriorating health of human crew while in transit. Not only are humans in zero-gravity for long periods of time, humans are also exposed to higher amounts of radiation. Five trajectory classes are discussed in this paper:

- Conjunction
- Free Return
- Mars-Earth Semicycler
- Earth-Mars Semicycler
- Cyler

A conjunction class trajectory can be the following:

- Direct trajectory
- Semidirect trajectory
- Stopover trajectory [11].

In a direct trajectory, spacecraft hardware fly directly from the surface of Earth to the surface of Mars without intermediary orbits [11]. In a semi-direct trajectory, spacecraft enter Martian orbit before descending to the surface [11]. In a stopover trajectory, spacecraft enter Earth orbit, then Martian orbit, before landing on the surface of Mars [11].

A free-return trajectory is designed such that if the spacecraft does not perform a Martian capture maneuver, the spacecraft will automatically return to Earth orbit with minimal maneuvers [11]. This is an ideal trajectory in case there is spacecraft failure within the propulsion system.

Mars-Earth semicycler, and Earth-Mars, semicycler orbits are similar in that both orbits involve orbiting one body while occasionally flying by the other [11]. For example, a Mars-Earth semicycler trajectory will have a spacecraft orbit Mars and perform maneuvers to fly by Earth when needed. However, in a cyclor orbit, the spacecraft will perpetually fly by both planets [11].

The report “An Examination of ‘The Martian’ Trajectory,” analyzes the trajectory of the spacecraft in the novel “The Martian” by Andy Weir. The reports purpose is to determine if the trajectory is in accordance with modern orbital dynamic theories. The spacecraft launches from Earth and enters Martian orbit where a surface team launches in a MAV to rendezvous with the transport spacecraft [12]. After the rendezvous the spacecraft leaves Martian orbit to return to the surface of Earth, but instead of landing, the spacecraft maneuvers for a flyby of Earth. The spacecraft then proceeds to a flyby of Mars to rendezvous with another astronaut launching from the surface [12]. While the spacecraft being analyzed in this report is fictional, the methodology and assumptions used for orbital dynamics can be applied to conceptual spacecraft designs. The first assumption is constant spacecraft acceleration such that thrust is automatically adjusted for the changing mass of the vehicle due to propellant burn off. The second assumption is that the Earth entry velocity does not exceed 11.5 km/s, similar to the velocity of crewed capsules used today [12]. The report found that the trajectory certainly follows the rules of physics. However, it does not address the issue of human endurance of heat and radiation while the spacecraft transits within Venus’ solar orbit [12].

Utilizing a hybrid propulsion system consisting of chemical and electrical components allows for more fuel-efficient Mars trajectories [13]. Efficient trajectories use either the chemical or electrical propulsion systems at various phases of flight, as discussed “Mars Hybrid Propulsion System Trajectory Analysis Part I,” [13]. This report focuses on using electric propulsions for long segments of the trajectory where minimal maneuvering is necessary such as the transit between Earth and Mars. However, chemical propulsion is used where large amounts of delta V is required, such as during launch, landing and leaving orbit. The benefit of such a system allows a single vehicle to complete a mission between Mars and Earth with minimal fuel and supply rendezvous [13]. This report defines multiple spacecraft trajectories that depart in 2033, 2039 and 2049 utilizing a hybrid propulsion system.

NASA’s Curiosity rover successfully landed on Mars in August of 2012. “2011 Mars Science Laboratory Reconstruction and Performance from Launch Through Landing,” analyzes the performance of the launch trajectory. The report compares the predicted and actual trajectories including maneuvers. In conclusion, the rover landed approximately 2.4 km from the predicted

landing site, and trajectory correction maneuvers were less than 5% off from what was expected [14]. This shows how robust modern orbital dynamic calculations have become.

The trajectories in “Interplanetary Trajectories,” discusses the various orbits and transfers that can be used to transport a spacecraft to and from Mars [15]. Topics also include methodology for a sensitivity analysis, as well as methods of planetary departure [15]. This textbook is a useful source to reconstruct sensitivity analyses discussed in previously mentioned technical reports.

1.1.4 Mission Logistics

Reducing logistical mass is a vital aspect of any crewed mission to Mars. Technologies are being studied that can reduce the mass of crewed mission necessities in “Exploration Mission Benefits from Logistical Reduction Technologies,” [16]. These necessities include clothing and waste disposal. Crew will also not be able to rely on mission control to determine the location of items onboard the spacecraft. Since there is a minutes-long delay in communication both ways, crew need to be able to find missing items without the support of mission control in the event of an emergency. A RFID inventory system is being investigated to be used on such long duration spacecraft missions [16]. In this report five technologies are being investigated:

- Clothing
- Reusable Cargo Bags
- Trash Management
- Sanitary Systems
- Autonomous Logistic Management Technologies [16]

A four-person crew requires 300 kg of clothing per year. Since there are no laundering services available on current spacecraft, crews must dispose of clothing when it is no longer acceptable for wear. By increasing the length of wear for each article of clothing to about 330 days, a break-even point is achieved where it is just as efficient to launch new clothes, rather than launder them in space [16]. Laundering in space also has the added logistical challenge of separating water from clothing fibers [16]. Cargo transport bags (CTB) can be reused as other materials on board spacecraft, such as:

- Sound dampening blankets
- Crew quarter partitions
- Trash storage

Reusing CTBs provide a weight savings of approximately 140 kg per year for every four crew members [16]. A heat melt compactor (HMC) can provide a way to microbially stabilize and compact trash [16]. A new universal waste management system (UWMS) was also investigated for use that is more compact in size and can more efficiently pretreat waste for water recovery [16].

The SLS is NASA’s primary launcher design for missions to the Moon and beyond. The SLS program faces many logistical challenges which include design, development, and manufacturing occurring at multiple sites throughout the United States. These challenges are discussed in “NASA Space Rocket Logistics Challenges,” [17]. Another challenge was mixing old

technologies with new technologies which created unique logistical challenges. Lessons learned from other programs show that considerations such as commonality, standardization, and reliability should be considered to mitigate logistical issues [17]. Supply chain responsibilities should also be strictly defined and a means for reporting real time demand for flight material should be utilized. RFID technologies to track inventories is also a suggestion to improve logistical efficiency.

The Asteroid Redirect Mission (ARM) seeks to send humans beyond low Earth orbit and to a nearby asteroid. This mission is discussed in “Logistics Needs for Potential Deep Space Mission Scenarios Post Asteroid Redirect Crewed Mission,” [18]. This mission is being investigated as a stepping stone for future missions to Mars. Since both an asteroid mission and a Mars mission are long duration, logistical concerns are similar. This report describes methods used to define consumption rates of various consumables required by a human crew as well as mass and volume requirements. These values can be used in calculating the mass requirements of a human mission to Mars. This report also includes consumption comparisons to lunar missions. Opportunities for improvement include reducing the hydration level of current foods provided to crew because food mass was up to 66% of the weight of all consumables [18].

Mars One was a Dutch startup company which intended to establish a colony on Mars. However, the technology that Mars One proposed was heavily scrutinized by industry professionals in “Comments on the MIT Assessment of the Mars One Plan.” The technology was found to be inadequate for a successful trip to Mars [19]. Logistical criticisms of the Mars One mission can be useful in identifying technology areas that require additional development [19]. Some of these criticisms include:

- Maintaining oxygen levels in the crew compartment while growing crops
- Advancing the TRL of technologies used to gather materials for fuel production
- Designing environmental control and life support systems (ECLSS) for micro and Martian gravity [19]

The mission operations chapter in “Space Mission Analysis,” provides details on developing mission operations plans. The chapter also describes logistical functions required for space missions. Important aspects to consider in space mission are the sizing of parameters and their related costs [20]. Automating certain functions between the spacecraft and mission control are also beneficial [20]. The step-by-step guidance in mission planning is in line with the methodology in previously discussed reports.

1.2 Literature Review Conclusions

The literature review establishes a baseline for the methodology of this project. At the system level, it is advantageous to execute a mixed design approach that borrows the best aspects of bottoms-up design and parametric design. It is also shown that a staged approach to lander systems, with interchangeable stages that serve different purposes, can be successfully utilized for Martian missions. A propulsion system with liquid methane and liquid oxygen as propellants is cited to be an effective system due to the ability to develop the propellants from the Martian

atmosphere. Other types of propulsion systems are still effective, but only methane and oxygen provide the landers with reusability. Traditional methods of orbital design have proven effective with minimal differences between theoretical and actual flight paths. Therefore, design methodology as discussed in technical reports and textbooks can be successfully applied to the design of this lander as well. Literature regarding mission logistics shows there are still many unknowns due to the intricacies of long-duration human spaceflight missions. Therefore, the estimates used for logistical mass in literature will also be used in this project design.

1.3 Project Objective

The objective of this project is to design a human-rated lander that can transport crew and cargo from the surface of Mars. The following components will be designed for a mission to Mars:

- A high-level subsystem architecture
- A detailed propulsion system
- Orbital trajectories
- Mission logistics

1.4 Methodology

Transportation spacecraft are currently being researched and developed that can land on the Moon and Mars. Although a project of this kind has been conceptualized many times, by multiple space agencies, a human-rated spacecraft landing on Mars has never been attempted. Therefore, there are many problems to solve to bring this concept to reality:

1. **Definition of system requirements:** A system-level design will be created that covers all the requirements for a human-rated spacecraft. Existing spacecraft, such as the Apollo Lunar Landers, will be used as a baseline. Conceptual spacecraft that are currently in the research and development phase in the Artemis program will also be considered.
2. **Propulsion system design and analysis:** The propulsion system will be designed based on landing systems that have already successfully flown on Mars. These will include technology from the InSight lander, and the Mars sky crane used for the Curiosity and Perseverance rovers. CFD analysis will be used to gauge the effectiveness of the spacecraft nozzles in the Martian atmosphere.
3. **Definition of orbital and re-entry dynamics:** A study of the most efficient transfer orbits will be considered and used to define the final Mars transfer orbit. A trade study on existing Martian re-entry will determine the most cost-effective means to transport all the required hardware and crew.
4. **Definition of program milestones and concept of operations:** The most effective means of conducting a development program and operating the Martian lander will be studied. Landing zones will be considered based on current NASA research for safe rover landing zones. Program benefits will also be studied.

Overall, the methodology for this project will include:

- a literature review of existing reports
- trade studies of existing and new technologies
- designs based on findings from literature and trade studies
- a performance analysis of the design
- suggestions for additional research and improvement.

Chapter 2: System Level Design of a Martian Lander for Crew and Cargo

The objective of this chapter is to design a reusable Martian Lander System at the system level that can transport crew and cargo to and from the Martian surface.

2.1 Preliminary Estimate of Mission Requirements and Constraints

Preliminary estimates for mission requirements and constraints are discussed in this section. The following aspects are compared and analyzed:

- Historical lander design data
- Existing launcher capabilities
- Future launcher capabilities

2.1.1 Historical Data

Historical data is limited for human lander systems. The Apollo program is the first and only program to successfully land humans on another celestial object. Six Apollo missions successfully landed humans on the moon with surface missions lasting up to 75 hours. However, only two distinct Apollo lander designs exist. Two designs do not provide enough historical data points on their own to advise future programs on design requirements for a Martian lander.

Theoretical lander designs, developed by NASA for missions beyond Apollo, are used to provide additional data points. The additional data will determine requirements for the system-level design of a new Martian lander. Two NASA lunar landers, the MSFC Vertical Lander, and the Lander Design Analysis Cycle-4 were designed to take a crew of four astronauts to the lunar surface for up to seven days [1]. The LDAC-4 went through multiple design cycles for hazard mitigation and performance improvements [1]. The LDAC-4 is a relatively matured design when compared to other theoretical lunar landers [1]. The NASA Mars Lander is also a relatively matured design that addresses the added complexity of landing through the Martian atmosphere.

The following table summarizes key characteristics of the flight-proven and theoretical landers that are discussed in this section.

Table 2.1 - Comparison of historical lander data [1]

Lander	Gross Mass [kg]	Diameter [m]	Height [m]	Crew	Surface Duration
Apollo 11	15,103	7.04	4.22	2	22 Hours
Apollo 17	16,447	7.04	4.22	2	75 Hours
MSFC Vertical Lander	49,972	8	9.5	4	7 Days
LDAC-4	44,318	9.1	10	4	7 Days

Lander	Gross Mass [kg]	Diameter [m]	Height [m]	Crew	Surface Duration
NASA Mars Lander	65,341	8	7	4	24 Hours

2.1.2 Current and Future Launcher Capabilities

Few operational launchers can send payloads on a Trans-Mars injection, TMI, orbit. The following list includes flight-proven launchers with TMI capabilities:

- Delta IV Heavy
- Atlas V
- Falcon Heavy

Two launchers currently under development, the Space Launch System, SLS, and Starship are also considered. SLS and Starship are late into the development cycle and completed multiple system-level tests. The following table lists currently available and planned launchers and compares critical performance characteristics required to develop a Martian lander.

Table 2.2 - Launcher comparison [21]

Launcher	Payload [kg]	Fairing Diameter [m]	Fairing Height [m]	Orbit
Saturn V	41,000	6.6	8.6	TLI
Delta IV Heavy	8,000	5.1	19.8	TMI
Atlas V	8,900	4.2	11	TMI
Falcon Heavy	16,800	5.2	13	TMI
SLS	45,000	10	27	TMI
Starship	100,000	9	18	TMI

2.1.3 Requirement and Constraint Analysis

Legacy landers from the Apollo era were relatively lightweight and designed for missions meant to last only a few days with a crew of two. Next-generation landers are designed for longer duration missions, up to seven days with a crew of four [1]. This greatly increased the complexity and mass of the landers which weighed in between 45,000 and 65,000 kilograms compared to a maximum of 16,000 kilograms of the Apollo landers [1]. The Apollo landers only consumed a portion of the total Saturn V payload capacity because all mission hardware was launched on a single flight. However, for future Lunar and Martian missions, multiple flights are planned to send all required hardware to orbit [1]. First, landers and other cargo are launched. Then, the crew is

launched to rendezvous in orbit. This allows lander designs to take advantage of the full launch vehicle payload capacity.

The Falcon Heavy has the largest payload capacity to TMI among all the flight-proven launchers [2]. However, with a payload capacity maximum of 16,800 kilograms, the Falcon Heavy is still incapable of flying a fully assembled modern lander. The SLS can launch a few modern lander designs, and Starship is capable of flying all of them. However, SLS and Starship are still in the development phase and are not guaranteed to be successful launchers. As a risk mitigation plan, the design of the Martian Landing System, MLS, will be constrained to be compatible with at least one flight-proven launcher.

Based on historical data and existing launcher capabilities, the MLS components will be constrained to the following requirements:

- Launch on a Falcon Heavy rocket
- Have a gross mass of 16,800 kg
- Must fit within a fairing that is 5.2 meters in diameter and 13 meters long

However, the MLS will also be designed to be flown as a complete assembly on future launchers such as the SLS and Starship.

2.2 Characterizing Mission Architecture and Concepts

2.2.1 Concept of Operations

The MLS consists of multiple segments that can be launched individually on a Falcon Heavy launcher or fully assembled on SLS or Starship. These segments include:

- A descent stage
- An ascent stage
- Cargo module
- Fuel module

The primary configuration of the MLS will consist of the descent stage and the ascent stage. The descent stage includes a deployable heat shield and retro rockets, and the ascent stage will contain the crew cabin. The ascent stage will be interchangeable with the cargo module and fuel module for the secondary configurations. The cargo module will contain supplies and hardware needed for surface missions. The fuel module will synthesize methane and oxygen from the Martian atmosphere to fuel both the ascent and descent stages after landing. Both the ascent stage and descent stage will have single stage to orbit, SSTO, capabilities. The fuel module will be based on a rover platform to allow for transportation to other landers for refueling. The ascent stage, descent stage, and cargo module are designed to be reusable, with the fuel module designed to remain on the surface.

Optimal launch windows from Earth to Mars, occur approximately every two years. The launch of MLS hardware will occur during one of these launch windows to minimize ΔV requirements. Creating fuel from the Martian atmosphere will take months [8]. Therefore, the first modules to land on the surface will be the fuel modules. A cargo module will be the next module to land with surface mission hardware and supplies. With all the necessary hardware for a surface mission successfully landed, a crewed capsule such as Orion, will transport the crew to rendezvous with an awaiting lander in Martian orbit.

The ascent module containing the human crew will be the last segment to reach the surface. The fuel modules will first fuel the ascent stage to return the human crew to Martian orbit. Then

the fuel module will refuel the descent stages and cargo modules which will return to orbit for reuse on later missions.

2.2.2 Subsystem Overview

The system-level design of the MLS contains the following subsystems:

- Propulsion
- Life Support
- Thermal
- Electrical
- Guidance, Navigation and Control, GNC
- Structures.

These subsystems are described at a high level in the following sections.

2.2.3 Propulsion

The propulsion subsystem will be designed with engines that are optimized for flight within the entire range of the Martian atmosphere to enable SSTO capabilities. Methane and oxygen are the ideal propellants for the propulsion system because these propellants can be produced from the Martian atmosphere and can be utilized in refueling operations. The propulsion system on the ascent stage, descent stage, and cargo modules will be designed to maximize commonality.

A detailed design of the propulsion system is included in Chapter 3 of this report. This includes the optimization of the engine nozzles, as well as CFD simulations to analyze the performance of the engine at varying altitudes. The preliminary requirement for the propulsion subsystem is to take 16,800 kg of dry mass into Martian orbit from the surface. The nozzle designed in Chapter 3 has a theoretical thrust capability of 2.42 MN.

2.2.4 Life Support

The life support system is only required on the ascent stage of the MLS. The life support system design will leverage existing designs from NASA's Orion crewed vehicle. The Orion spacecraft is also capable of supporting a crew of four, and it is currently in the production phase for use in NASA's Artemis program. The life support subsystem provides an earth-like atmosphere, potable water, protection from radiation and the Martian environment, and a waste containment system. The preliminary requirement is to independently sustain a crew of four for up to 7 days.

2.2.5 Thermal

The thermal subsystem will maintain the temperature of all MLS segments to stay within operating temperature requirements. The heat shield required for entry into the Martian atmosphere is also part of the thermal subsystem. Two technologies for a deployable heat shield are currently under investigation by NASA: the Hypersonic Inflatable Aerodynamic Decelerator, HIAD; and Adaptive Deployable Entry and Placement Technology, ADEPT [8]. These two technologies are not flight-proven, but these technologies will be utilized in the design of the MLS. A preliminary

design of the heat shield subsystem is included in Chapter 5 of this report. Due to computer hardware limitations, a simulation of heat shield reentry dynamics could not be performed.

2.2.7 Guidance, Navigation, and Control

GNC technologies from the Orion spacecraft and NASA's Mars Lander will be leveraged for use on the MLS. The GNC subsystem will control the reaction control system, RCS, and the main engines on the ascent stage, descent stage, and cargo module.

A detailed design of orbital trajectories is included in Chapter 4 of this design report. Trade studies between different orbits and an analysis of ΔV requirements are also included. A semi-direct interplanetary Hohmann transfer is determined to be the most effective trajectory.

2.2.8 Structures

The base structure of the ascent stage, and cargo module will be designed with commonality in mind. The substructures of the propulsion system will also be common among the ascent stage, descent stage and cargo module. The structure of the fuel module will be unique since it will be integrated with a rover base to facilitate ease of movement to landers on the Martian surface. Typical lightweight alloys of aluminum and titanium will be used for the structures and substructures of the MLS.

2.3 N2 Diagram and Requirements

This section includes a N2 diagram to show the interdependencies of each subsystem. Preliminary requirements are also summarized in this section.

2.3.1 N2 Diagram

The following figure is a N2 diagram of the MLS subsystems created in Simulink.

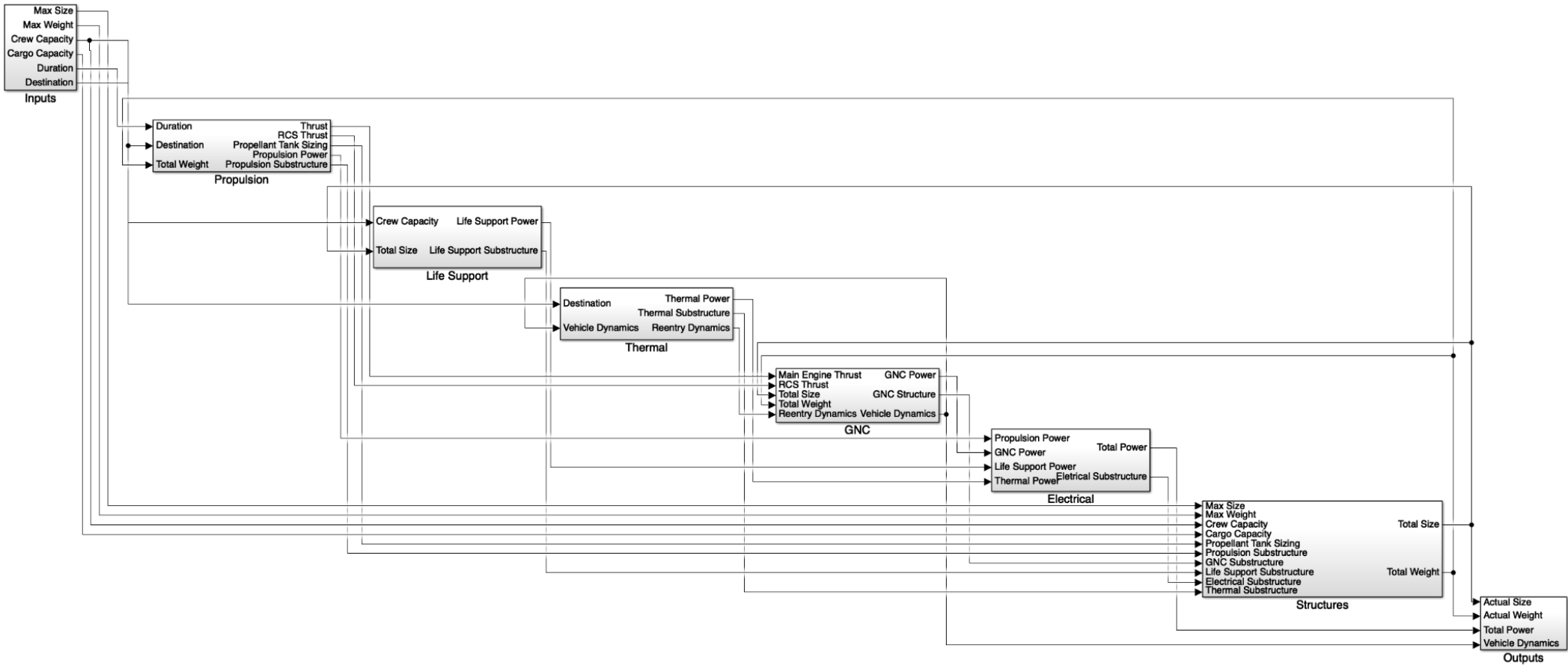


Figure 2.1 - N2 diagram

2.3.2 Requirements

The following table summarizes the key requirements of the MLS.

Table 2.3 - Preliminary MLS requirements

Category	ID	Requirement	Rational
Propulsion	1.1	Shall launch 16,800 kgs from the Martian surface to Martian orbit.	16,800 kgs is the maximum dry weight of a Falcon Heavy payload.
	1.2	Shall use methane and oxygen as propellants.	Methane and oxygen can be produced from the Martian atmosphere.
	1.3	Shall have refueling capabilities.	Refueling of the propulsion system is required to make the spacecraft reusable.
Life Support	2.1	Shall support 4 crew members for up to 7 days.	Historical data for modern lander designs shows 4 crew members and 7 days are common targets.
	2.2	Shall include redundant backup systems.	Life support is critical crew health and mission success.
Thermal	3.1	Shall utilize deployable heat shields.	Human landers require a heat shield that is far larger than the fairing diameter of any existing or planned launcher.
	3.2	Heat shields shall be reusable.	Non-reusable heat shields will add complexity to the system.
	3.3	Shall reduce velocity from hypersonic to supersonic speeds	The heat shield must slow down the spacecraft for the propulsion system to successfully fire.
GNC	4.1	Shall be capable of controlling the spacecraft from launch on Earth through landing on Mars and back to Mars orbit.	Avionics are required to accurately control the spacecraft and maintain the established trajectory.
Electrical	5.1	Shall provide enough energy to power all spacecraft subsystems.	All subsystems require electrical power to operate.

Category	ID	Requirement	Rational
Structures	6.1	Shall have a segment dry mass of no more than 16,800 lbs.	16,800 kgs is the maximum dry weight of a Falcon Heavy payload.

Chapter 3: Propulsion Subsystem Design

The propulsion subsystem is a critical component of the Martian Landing System. Historical data was reviewed to determine a trend for rocket engines of similar purpose.

3.1 Historical Data and Analysis

Historical data shows that a Specific Impulse value between 200 and 380 is typical values for rocket engines. Bi-propellant engines tend to have specific impulses that are on the higher end of this range. The thrust specifications of various engines do not yield a uniform trend across historical data points. However, newer engines such as the Raptor and RS-25 engines are both well above 2 MN of thrust. Both these engines have successfully flown in vacuum environments and thus are well suited as a baseline for a Martian Lander.

Table 3.1 - Historical propulsion data [21]

Propulsion System	Fuel/ Oxidizers	Engines	Thrust [N]	Dry Mass [kg]	Specific Impulse [s]	Propellant Mass [kg]
Apollo 11 Descent Stage	N ₂ O ₄ / Aerozine 50	1	80,068.4	2,034	311	8,248
Apollo 11 Ascent Stage	N ₂ O ₄ / Aerozine 50	1	23,130.9	2,445	311	2,376
MSL Sky Crane (Aerojet MR-80B)	Hydrazine	8	3,100 N	1,370	225-200	387
NASA Mars Lander	LCH ₄ /LOX	8	100,000	50,597	360	13,774
Falcon 9 Upper Stage (Raptor)	LCH ₄ /LOX	1	2,300,000	8,000	380	92,670
STS (RS-25)	LH ₂ /LOX	3	2,279,000	78,000	366	730,000

3.2 Nozzle Design

The design of the nozzle begins with establishing requirements. The initial requirements for the engine propulsion system are a specific impulse, I_{sp} , of between 200 and 350 seconds, and a thrust of between 1.5 and 2.5 MN. These values are in line with the historical data of propulsion systems of a similar purpose. Other requirements are based on physical size. The constraints are to be less than 5 meters in length and less than 2 meters in diameter. This size allows a two-stage configuration with the same engines can fit within the payload fairings of either SLS or Starship. These design parameters are summarized in the following table.

Table 3.2 - Engine design parameters

Design Parameters	Min	Max
Specific Impulse, I_{sp} [sec]	200	350
Thrust, T [N]	1.5×10^6	2.5×10^6
Length, L_N [m]	1	5
Diameter, A_e	0.5	2

To design the nozzle, isentropic flow is assumed for an ideal gas, meaning the flow is reversible and no shocks are present within the system. A mixing ratio, O/F , of 3.2 is defined in literature as an ideal ratio for liquid methane and liquid oxygen [8]. Methane and oxygen are both considered ideal gases at low temperatures. However, at combustion temperatures, the propellants no longer have a constant specific heat ratio, γ . Specific heat ratios at a certain temperature, T , are calculated in Eq. (3.1) where γ_{perf} is the specific heat ratio of an ideal gas at standard temperature and Θ is 3055 K (5500 Rankine) [22]. The final specific heat ratio, γ , is calculated by taking the ratio of the two specific heat ratios with respect to the mixing ratio, O/F , in Eq. (3.2).

$$\gamma_{gas} = 1 + \frac{\gamma_{perf} - 1}{1 + (\gamma_{perf} - 1) \left[\left(\frac{\Theta}{T} \right)^2 \frac{e^{\Theta/T}}{(e^{\Theta/T} - 1)^2} \right]} \quad (3.1)$$

$$\gamma = \frac{\left(\frac{O}{F} \right) \gamma_{oxygen} + \gamma_{methane}}{\left(\frac{O}{F} \right) + 1} \quad (3.2)$$

The combined fluid is then assumed to be an ideal gas and the specific heat ratio calculated by Eq. (3.2) is assumed to be constant. This means throughout the flow, the temperature variations do not have a significant effect on the specific heat ratio, γ . This is true as total temperatures between 2500 and 4000 K yield a specific heat ratio of ~ 1.26 . Combustion temperatures are initially set to 3500 K which is typical for engines of this size according to historical data.

Assuming ideal gas allows us to use the following isentropic flow relations to determine exit temperature, exit pressure, and area ratio with Eqs. (3.3-3.5) [23].

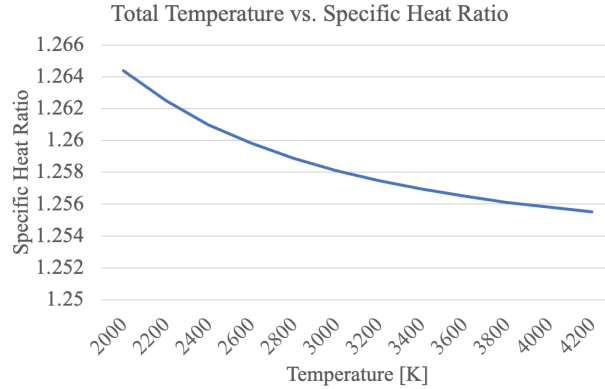


Figure 3.1 - Specific heat ratio plot

$$\frac{A_e}{A^*} = \left(\frac{\gamma + 1}{2}\right)^{-\frac{\gamma+1}{2(\gamma-1)}} \frac{(1 + \frac{\gamma-1}{2}M_e^2)^{\frac{\gamma+1}{2(\gamma-1)}}}{M_e} \quad (3.3)$$

$$\frac{T_e}{T_t} = \left(1 + \frac{\gamma-1}{2}M_e^2\right)^{-1} \quad (3.4)$$

$$\frac{P_e}{P_t} = \left(1 + \frac{\gamma-1}{2}M_e^2\right)^{-\frac{\gamma}{\gamma-1}} \quad (3.5)$$

Eqs. (3.6-3.8) are used to calculate exit velocity, thrust, and specific impulse to verify that the calculated values meet the original design parameters [23]. A high area ratio of greater than 40 is typical for nozzles that operate in or near-vacuum according to historical data. However, for a minimum length nozzle, the length of just the divergent section is well beyond size constraints for the engine. Area ratios less than 4 provide a minimum length of less than 5. To ensure there is sufficient margin for the combustion chamber and divergent section, area ratios of less than 3.2 are investigated further.

$$v_e = M_e \sqrt{\gamma R T_e} \quad (3.6)$$

$$F = \dot{m} v_e + (p_e - p_0) A_e \quad (3.7)$$

$$I_{sp} = \frac{F}{\dot{m} g_0} \quad (3.8)$$

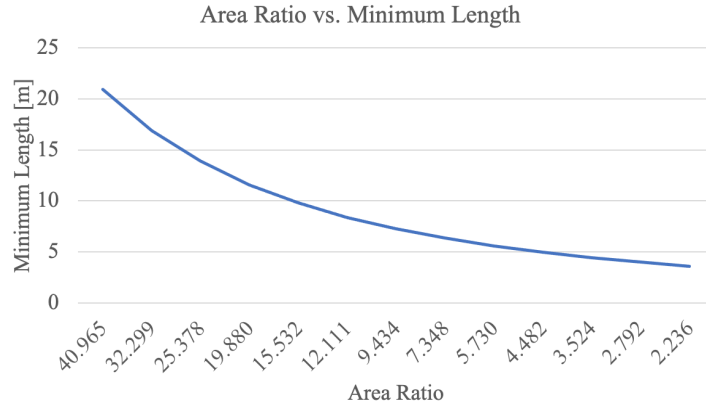


Figure 3.2 - Minimum nozzle length verification plot

Calculating the specific impulse for the acceptable range of area ratios shows area ratios greater than 1 can meet the specific impulse requirement of between 200 and 350 seconds. An area ratio of 2.494 is selected for further investigation which corresponds with an exit Mach number of 2.3.

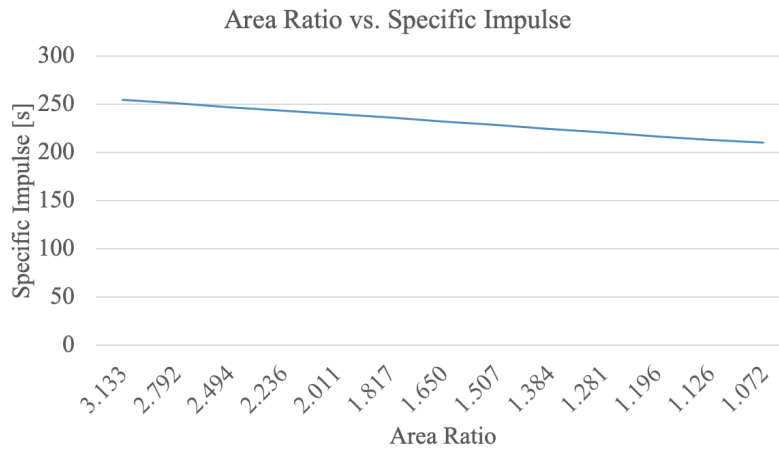


Figure 3.3 - Specific impulse verification plot

The remaining parameter to validate is the chamber pressure. The chamber pressure is varied from 0.5 to 6 MPa. Chamber pressures above 2.5 MPa result in thrust equivalent to at least 1.5 MN which meets the original design requirements.

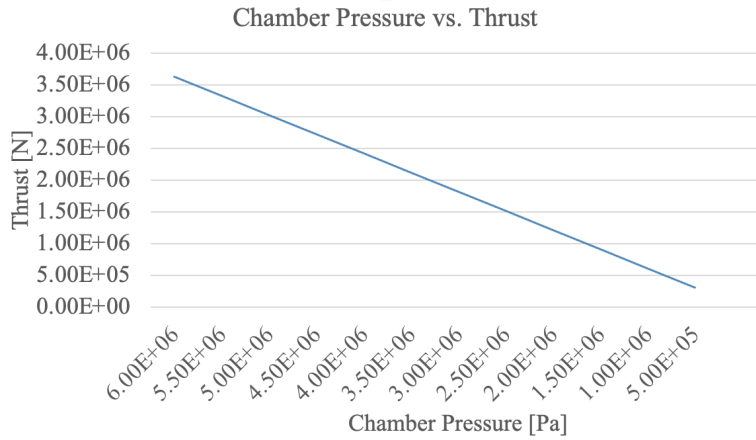


Figure 3.4 - Thrust verification plot

The final engine parameters are summarized in the following table.

Table 3.3 - Propulsion parameters

Propulsion Parameter	Value
Mixing Ratio, O/F	3.2
Specific Heat Ratio, γ	1.257
Atmospheric Pressure, P_0	600 Pa
Chamber Pressure, P_t	4 MPa
Exit Pressure, P_e	0.316 MPa
Chamber Temperature, T_t	3500 K
Exit Temperature, T_e	2084 K
Exit Diameter, A_e	2 m
Throat Diameter, A^*	.4 m
Mass Flow Rate, \dot{m}	997 kg/s
Exit Mach Number, M	2.3
Exit Velocity, V_e	2110 m/s
Thrust, F	2.42 MN
Specific Impulse, I_{sp}	248 s

The method of characteristics is used to determine the minimum length nozzle needed to ensure straightened flow within the divergent section of a nozzle. This is advantageous to avoid oblique shock reflections that could stall the flow within the engine. For simplicity, the 2D method of characteristics is assumed to provide the same nozzle contour as the 3D axisymmetric method of characteristics. The method of characteristics begins with determining the specific heat ratio of the fluid, 1.257, and the design exit Mach number, 2.3. These initial parameters are used in the Prandtl-Meyer function to calculate the maximum turning angle of the flow θ_{max} . These are Eqs. (3.9) and (3.10), respectively [24].

$$\nu = \sqrt{\frac{\gamma + 1}{\gamma - 1}} \tan^{-1} \sqrt{\frac{\gamma - 1}{\gamma + 1} (M^2 - 1)} - \tan^{-1} \sqrt{M^2 - 1} \quad (3.9)$$

$$\theta_{max} = \frac{\nu(M_e)}{2} \quad (3.10)$$

Since θ_{max} is the furthest the flow can turn away from itself without flow separation from the nozzle wall, the first wall point can be defined to be equal to θ_{max} . Individual Mach lines within the Prandtl-Meyer angle expansion fan and the interactions with other Mach lines define the “characteristic lines” in this method. The number of characteristic lines can be arbitrarily chosen. Typically, a minimum of seven characteristics provides a fairly accurate nozzle contour, but ten characteristics will be used for this design. The initial angles of each characteristic emanating from the turning point at the throat, are equal to θ_{max} divided by the number of characteristics. The intersection of each characteristic line is solved for flow angle, θ , by calculating Mach Number, Mach Angle, and Prandtl-Meyer Angle. Eq. (3.9) and the following equations show that only two of the intersection point values are needed to solve the other two.

$$K- = \theta + \nu \quad (3.11)$$

$$K+ = \theta - \nu \quad (3.12)$$

$$\theta = \frac{1}{2} [(K-) + (K+)] \quad (3.13)$$

$$\nu = \frac{1}{2} [(K-) - (K+)] \quad (3.14)$$

The relationship among points along left-running characteristics and right-running characteristics is defined by Eqs. (3.11) and (3.12) [25]. These values remain constant for all points along a left and right running characteristic. The characteristic line angles are defined by Eqs. (3.15) and (3.16) and shown in Figure 6 [25]. Initial conditions for intersection points 1 through 10 are defined as θ_{max} divided by 10. These values are both the flow angle, θ , and the Prandtl-Meyer angle, ν .

$$C- = \frac{1}{2} (\theta_1 + \theta_3) - \frac{1}{2} (\mu_1 + \mu_3) \quad (3.15)$$

$$C_+ = \frac{1}{2}(\theta_2 + \theta_3) + \frac{1}{2}(\mu_2 + \mu_3) \quad (3.16)$$

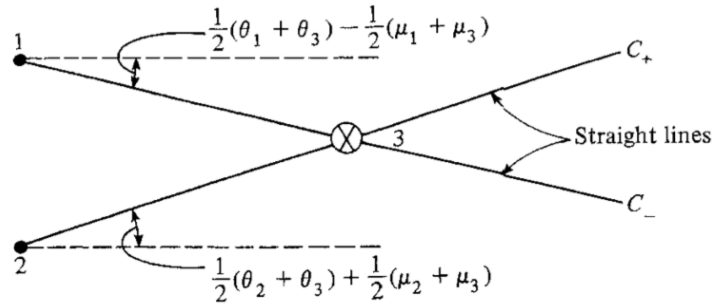


Figure 3.5 - Intersection point diagram [25]

Solving for each point by the method of characteristics by hand is a laborious and error-prone task. Therefore, online calculators can be leveraged to accurately solve for each intersection point [26]. Figure 6 shows the characteristic lines for the divergent nozzle section with only select points labeled for clarity.

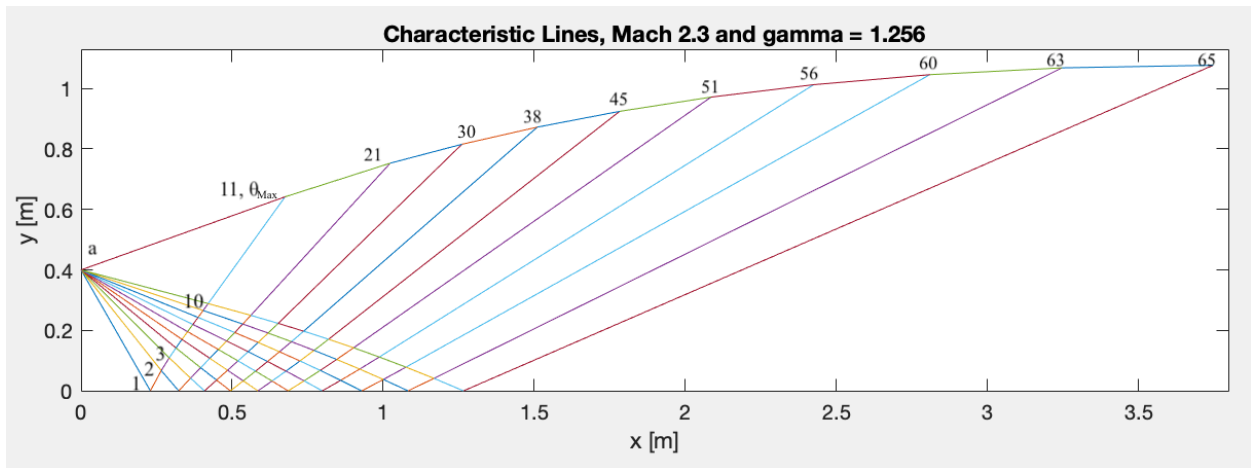


Figure 3.6 - Characteristic lines

The combustion chamber and the convergent section of the nozzle are arbitrarily defined as shown in Figure 7. There is no means to define the contour of the convergent nozzle section because the only critical aspect is that it converges to the throat diameter as defined by the area ratio. The combustion chamber is also selected to be of arbitrary size for simulation purposes.

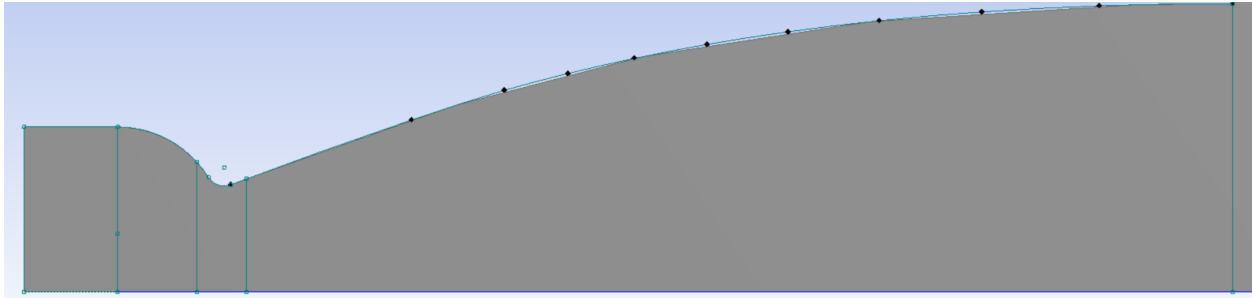


Figure 3.7 - Nozzle geometry

3.3 CFD Analysis

Computational Fluid Dynamics, CFD, simulations are conducted using Ansys Fluent. Simulations are used to verify the nozzle contour and design parameters defined in Section 3.2. Due to the limitations of Ansys Fluent, the exhaust plume of the nozzle cannot be simulated at the near-vacuum environment of Mars at a pressure of 600 Pa. Therefore, simulations of the nozzle are conducted starting at 101,325 Pa and decreased in increments to 6,000 Pa.

3.3.1 Geometry

The simulation geometry is defined by adding a 10 meter high by 30 meter long volume at the exit of the nozzle. This is shown in Figure 8. Note that Ansys Fluent only requires half of the geometry to be defined for axisymmetric simulations.



Figure 3.8 - Simulation geometry

3.3.2 Meshing

A structured mesh with quadrilaterals is chosen for this simulation. A structured quadrilateral mesh is ideal because it leads to high quality mesh with orthogonality and skewness of each element exceeding target values. Figures 3.9 and 3.10 show the mesh designed for the following simulations.

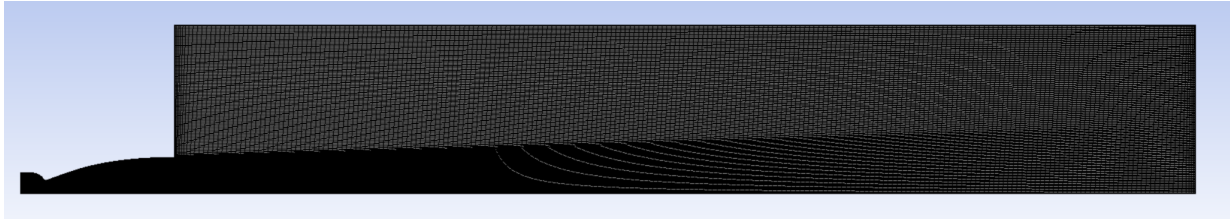


Figure 3.9 - Mesh

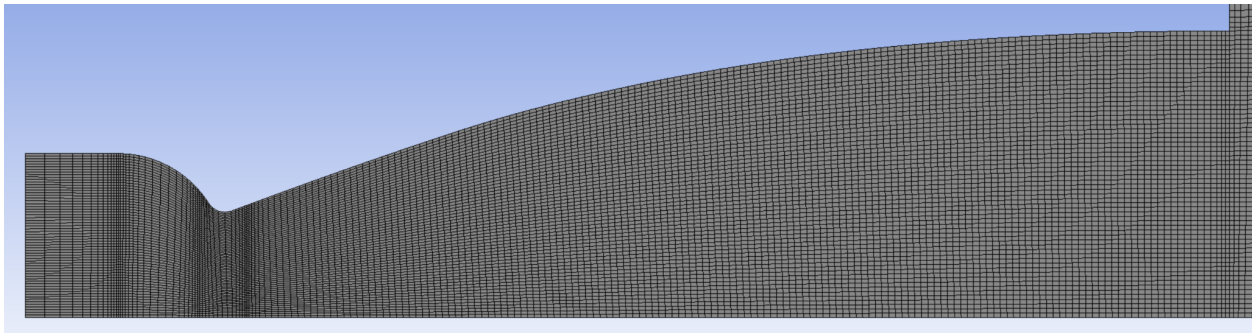


Figure 3.10 - Nozzle mesh

The target skewness value is 0.9 or lower, and the target for orthogonality is 0.9 or higher. Figures 3.11 and 3.12 are plots that show the Skewness and Orthogonality metrics. All elements are well within target values which proves the mesh is of high quality and is likely to lead to successful and accurate simulations. Table 3.4 summarizes the quality metrics.

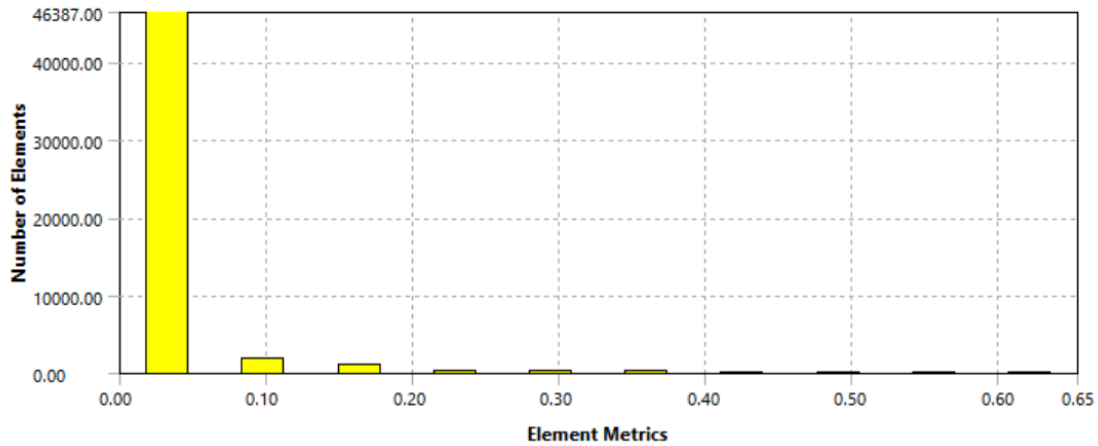


Figure 3.11 - Skewness metrics

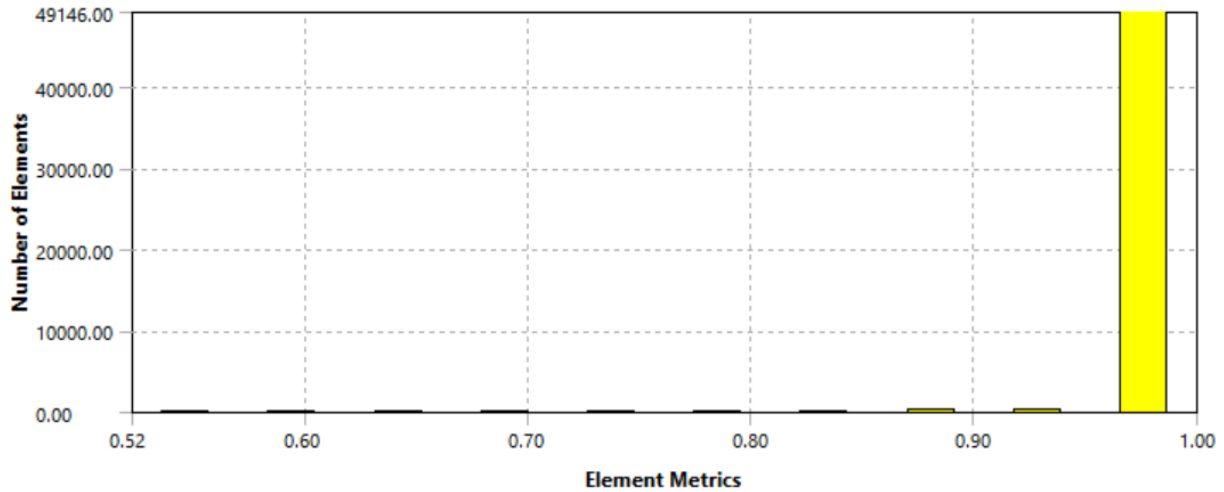


Figure 3.12 - Orthogonality metrics

Table 3.4 - Quality metric summary

Quality Metric	Target	Minimum	Maximum	Average
Skewness	< 0.9	1.5942×10^{-5}	0.65464	4.7983×10^{-2}
Orthogonality	> 0.9	0.52173	1	0.99489

3.3.3 Simulations

Simulations were conducted with the RNG, k-epsilon viscous model with energy. Fluid properties were adjusted to be an ideal gas with a specific heat ratio of 1.257. The fluid was assumed to be pre-combusted, and combustion settings were not enabled. The inlets and outlet boundary conditions were defined as pressure inlets and pressure outlets, respectively. Simulations were started at the sea level of Earth and slowly decreased to near-vacuum to better simulate the Martian atmosphere. Inlet pressure was set to 4 MPa, and temperature set to 3500 K. The following figures are the Mach number contours, pressure contours, and residual plots for the simulations.

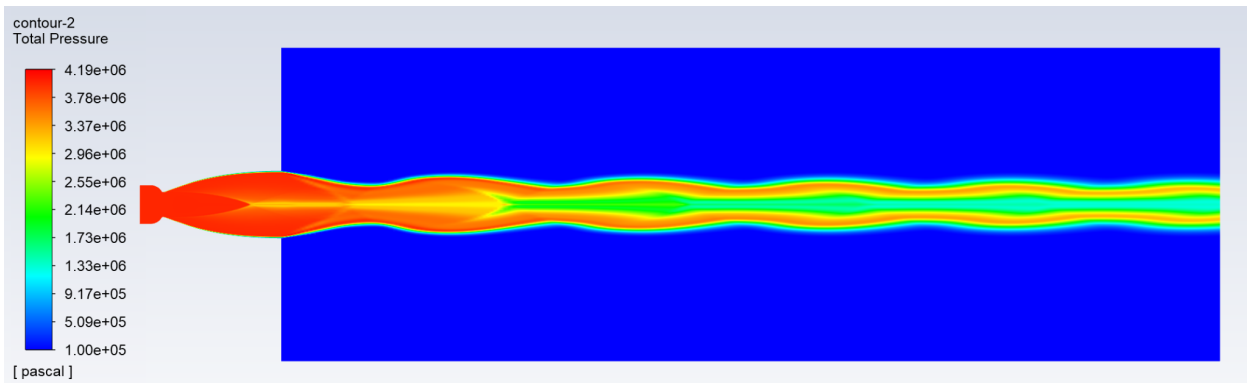


Figure 3.13 - Pressure contour for $P_0 = 101,325 \text{ Pa}$

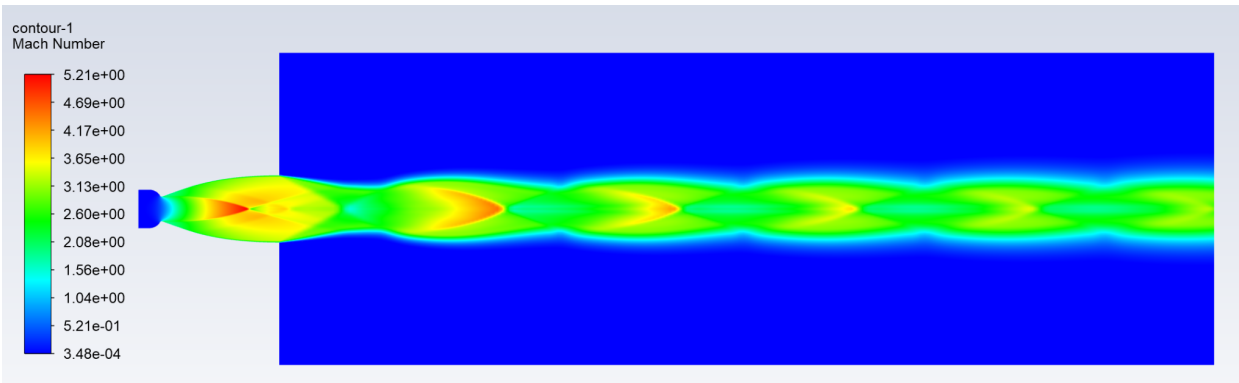


Figure 3.14 - Mach number contour for $P_0 = 101,325$ Pa

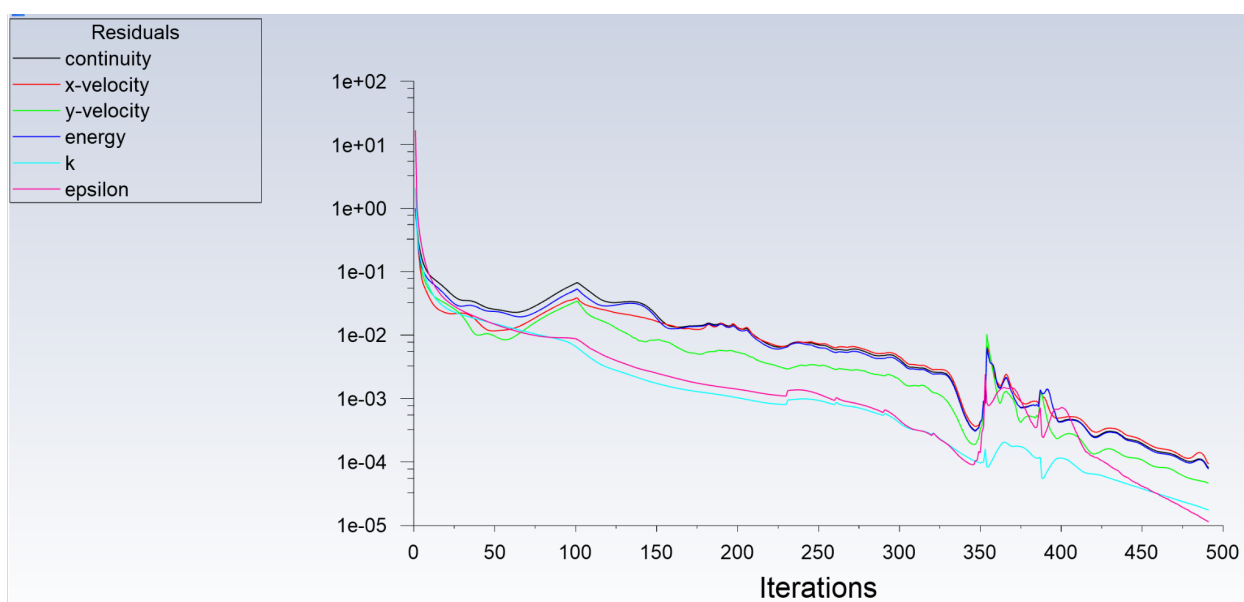


Figure 3.15 - Residuals for $P_0 = 101,325$ Pa

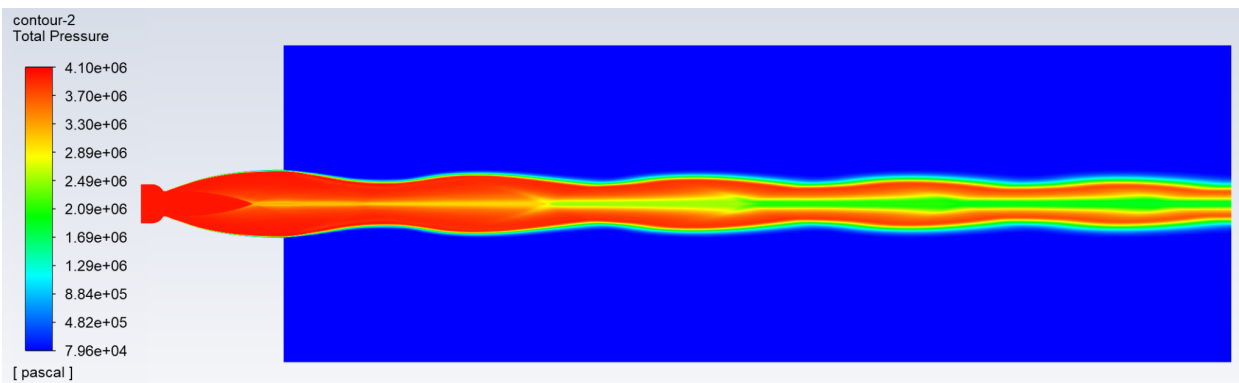


Figure 3.16 - Pressure contour for $P_0 = 80,000$ Pa

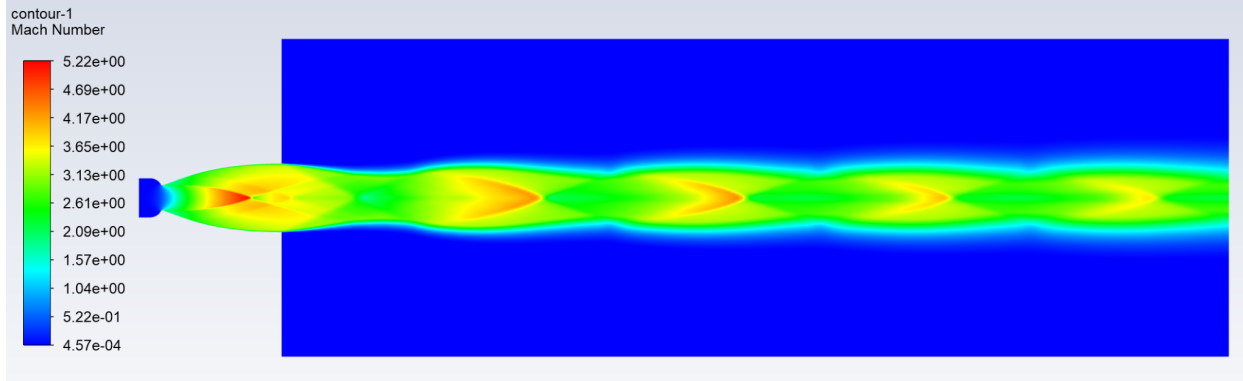


Figure 3.17 - Mach number contour for $P_0 = 80,000$ Pa

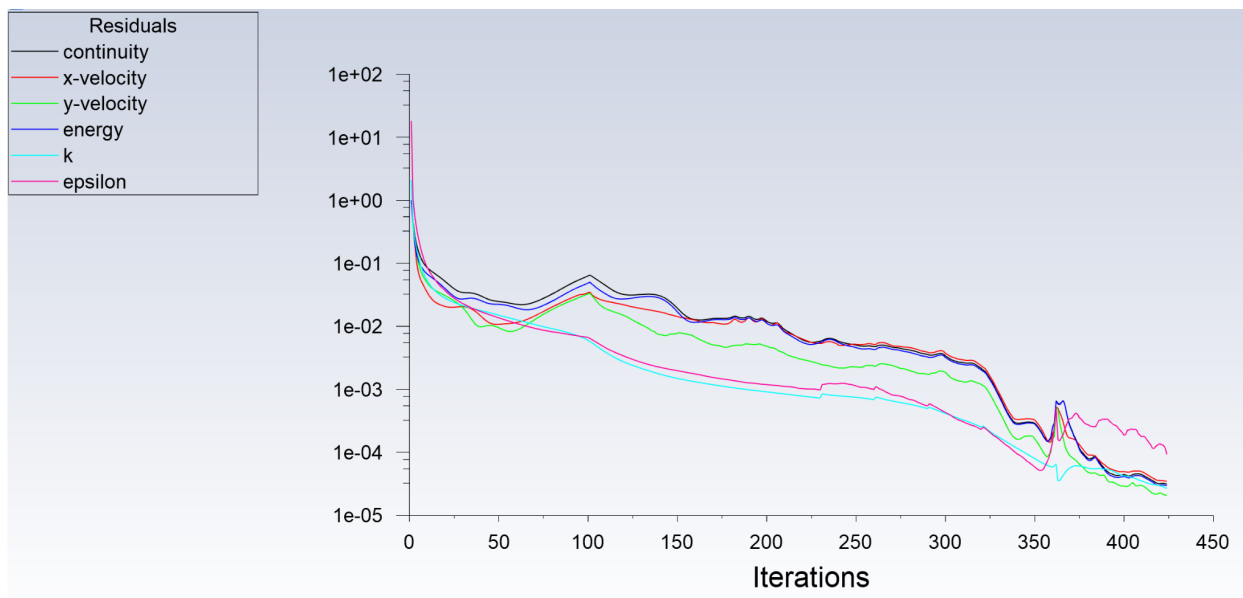


Figure 3.18 - Residuals for $P_0 = 80,000$ Pa

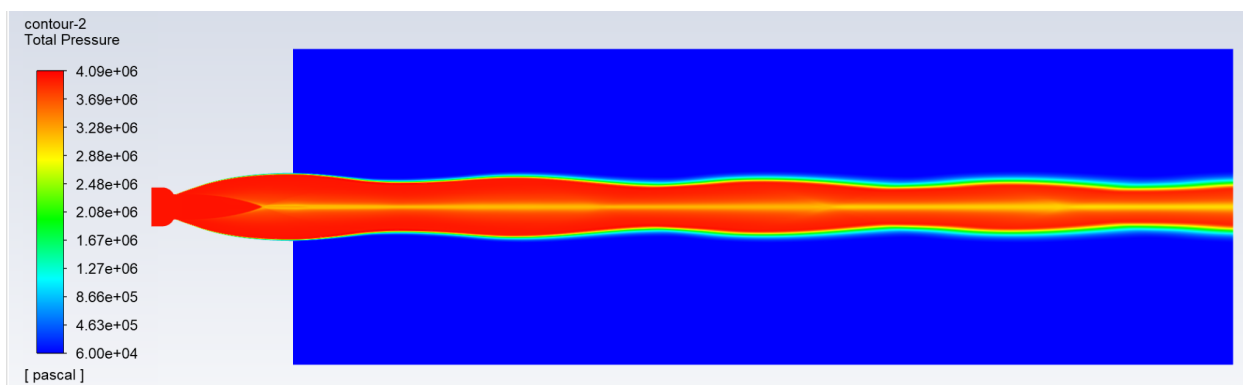


Figure 3.19 - Pressure contour for $P_0 = 60,000$ Pa

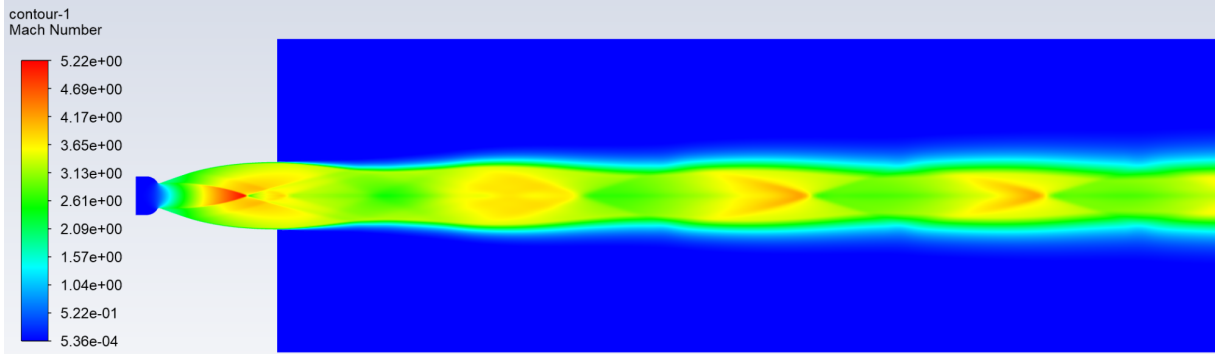


Figure 3.20 - Mach number contour for $P_0 = 60,000$ Pa

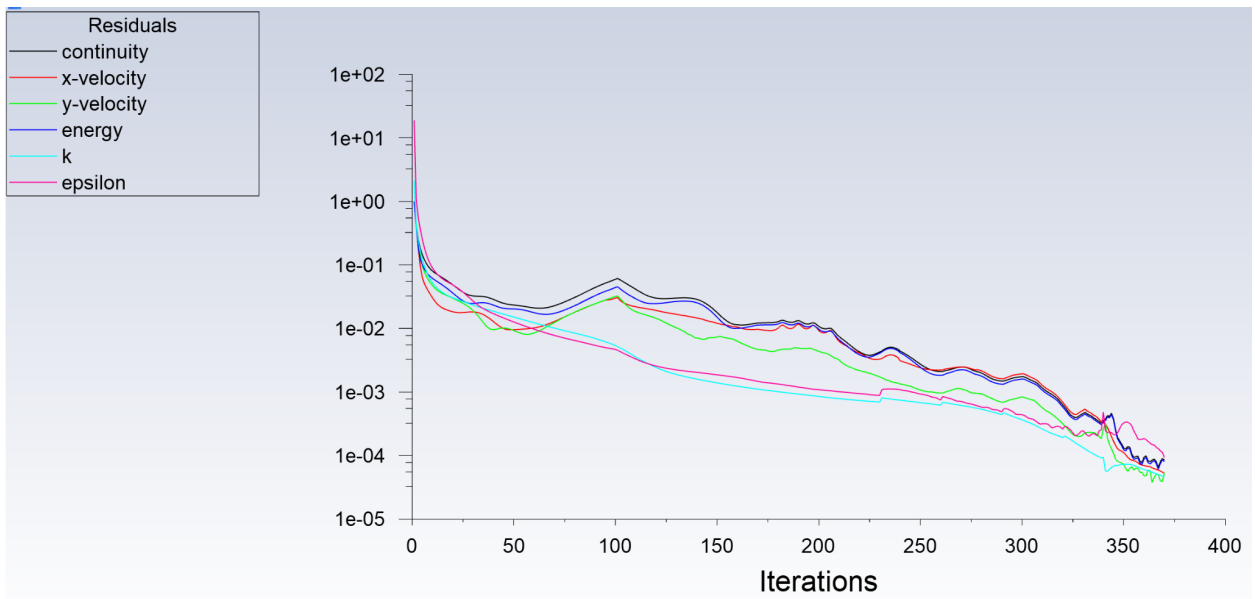


Figure 3.21 - Residuals for $P_0 = 60,000$ Pa

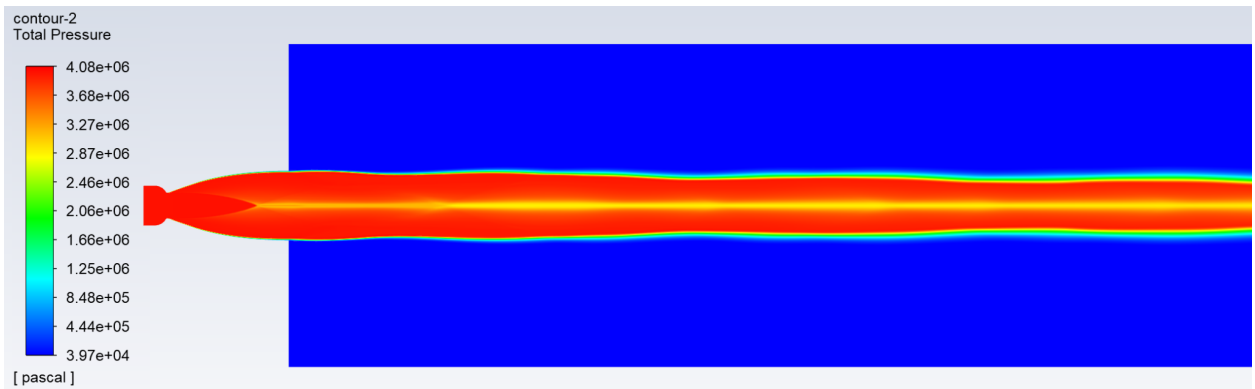


Figure 3.22 - Pressure contour for $P_0 = 40,000$ Pa

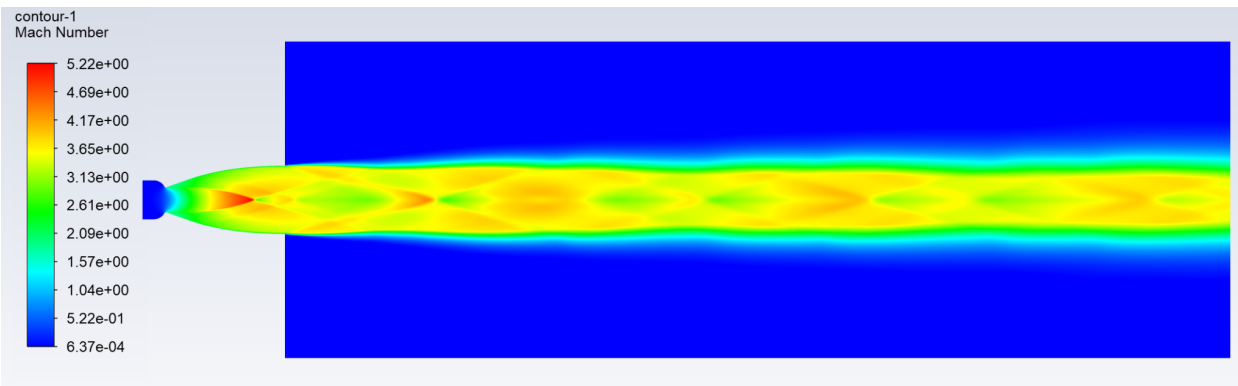


Figure 3.23 - Mach number contour for $P_0 = 40,000$ Pa

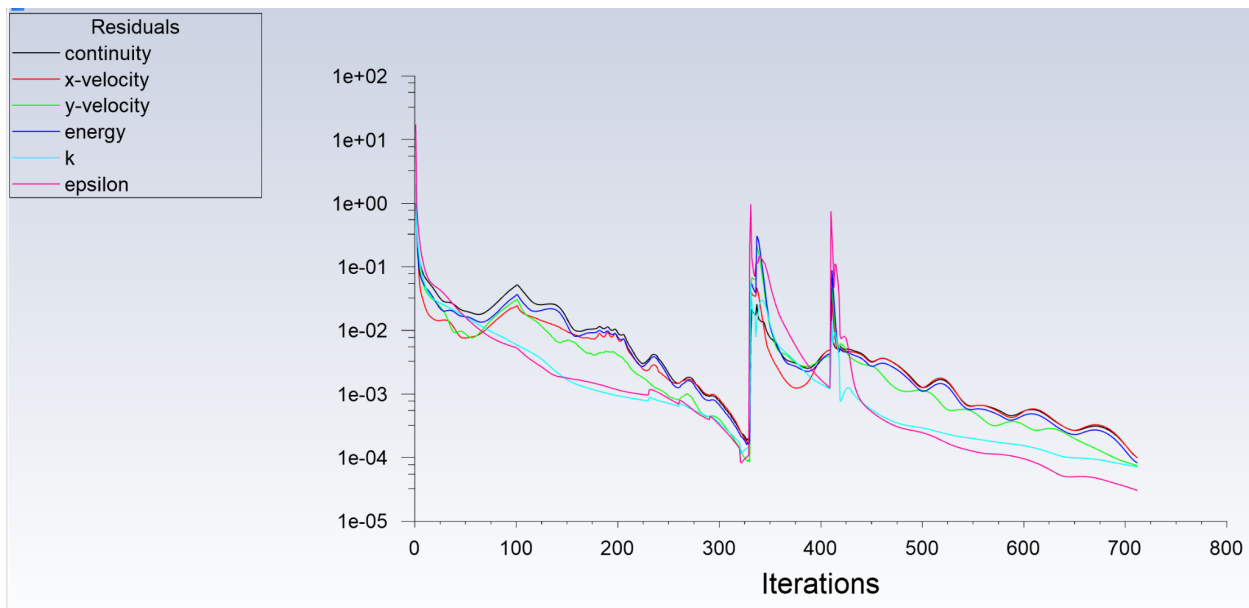


Figure 3.24 - Residuals for $P_0 = 40,000$ Pa

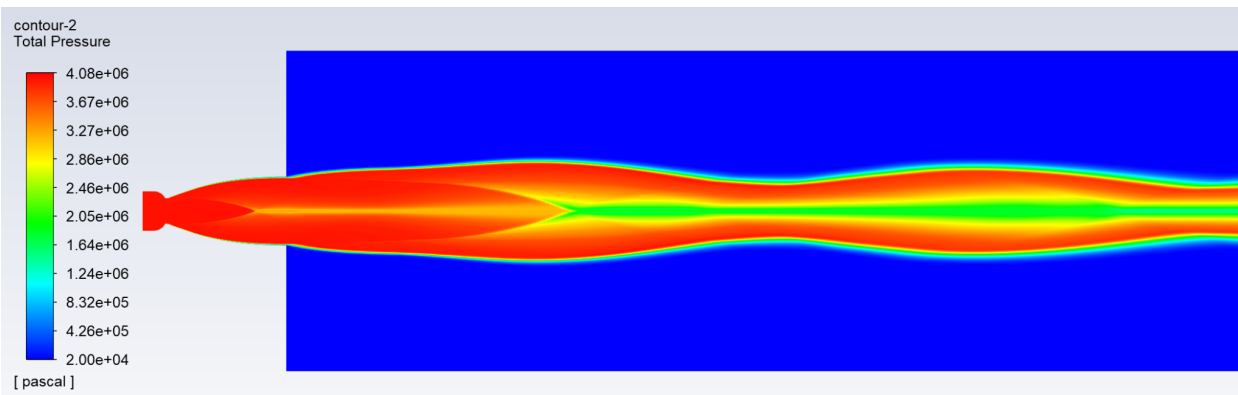


Figure 3.25 - Pressure contour for $P_0 = 20,000$ Pa

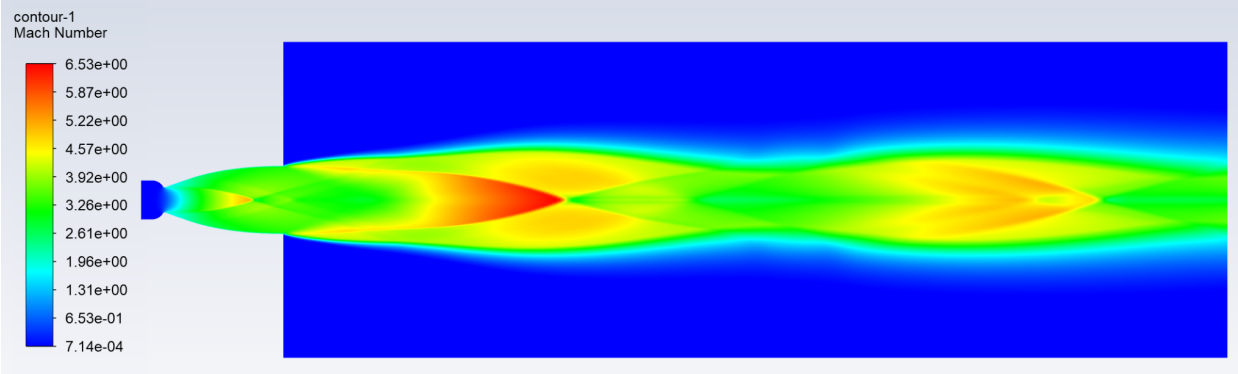


Figure 3.26 - Mach number contour for $P_0 = 20,000$ Pa

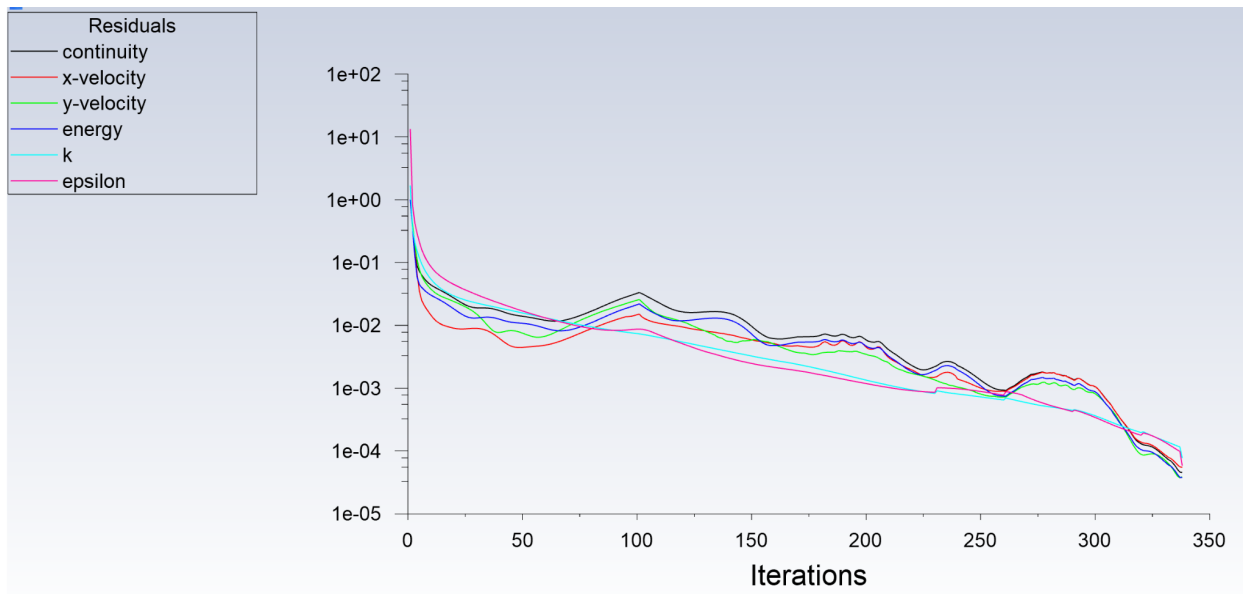


Figure 3.27 - Residuals for $P_0 = 20,000$ Pa

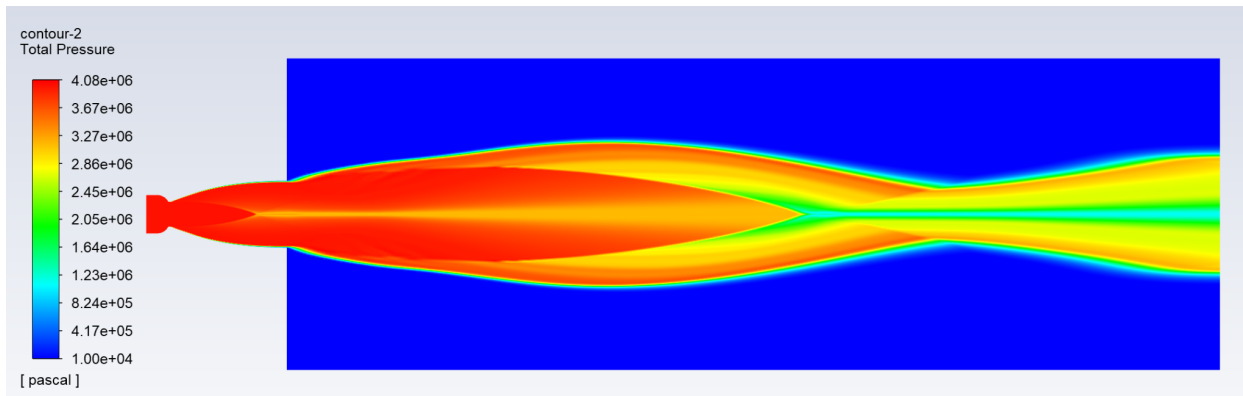


Figure 3.28 - Pressure contour for $P_0 = 10,000$ Pa

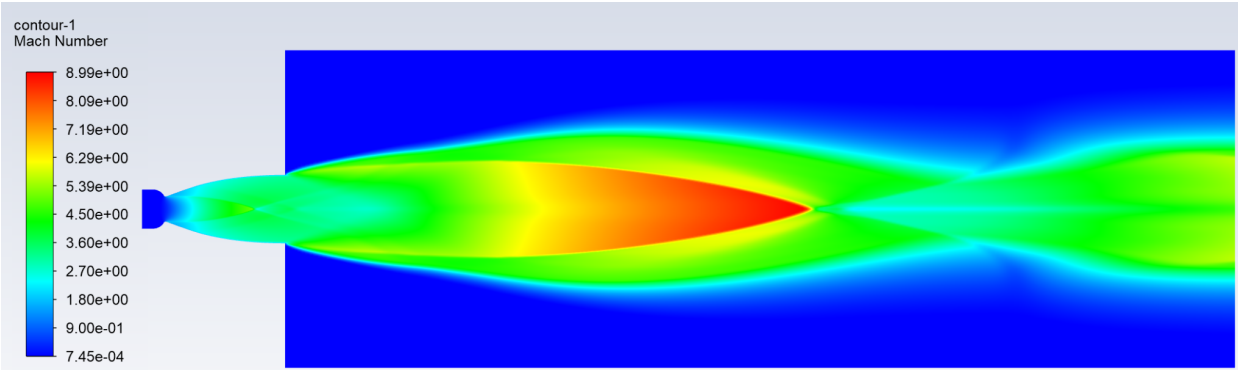


Figure 3.29 - Mach number contour for $P_0 = 10,000$ Pa

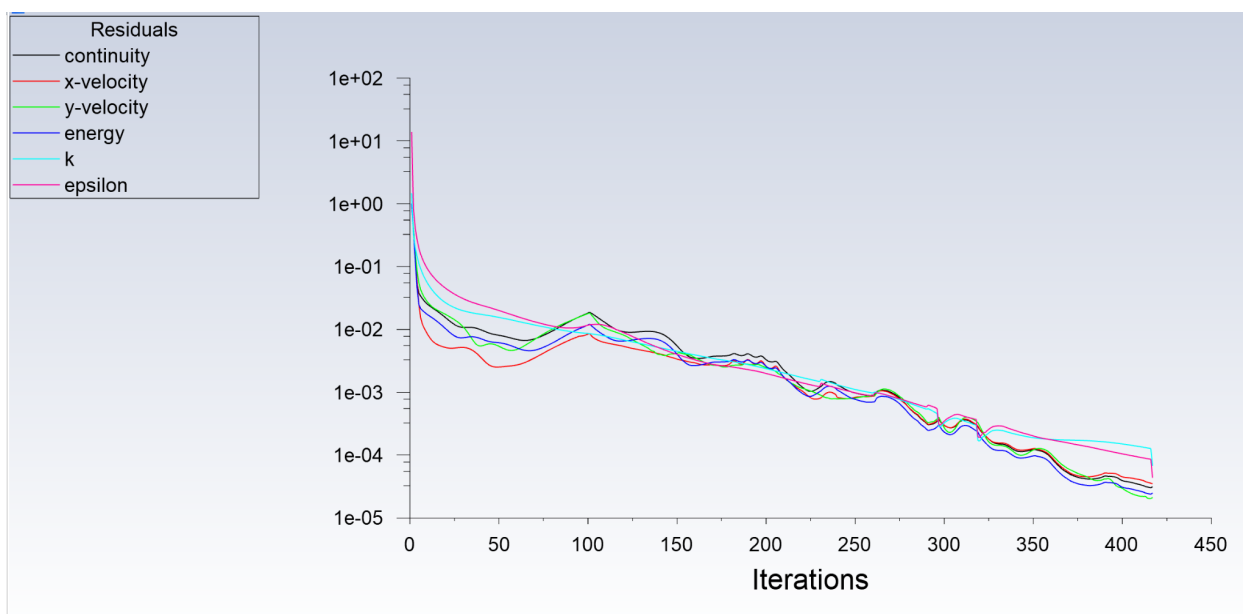


Figure 3.30 - Residuals for $P_0 = 10,000$ Pa

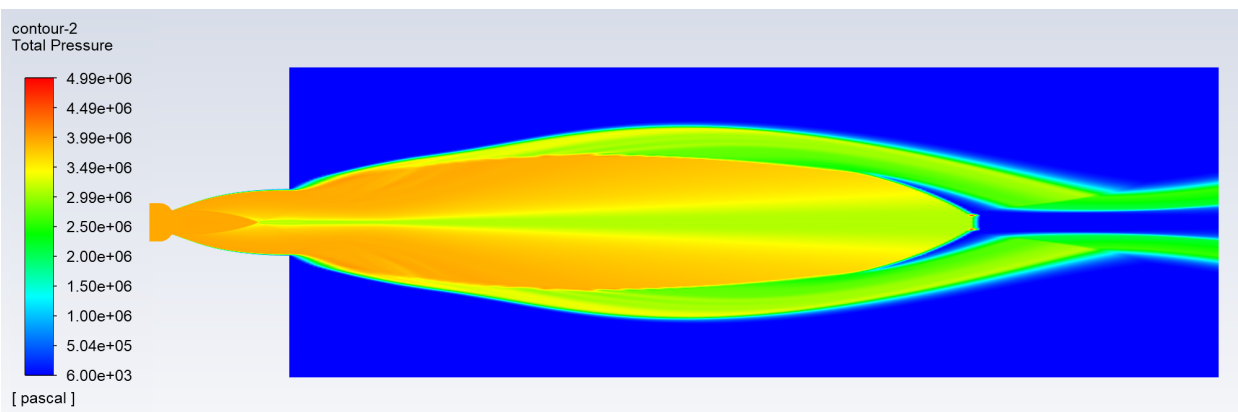


Figure 3.31 - Pressure contour for $P_0 = 6,000$ Pa

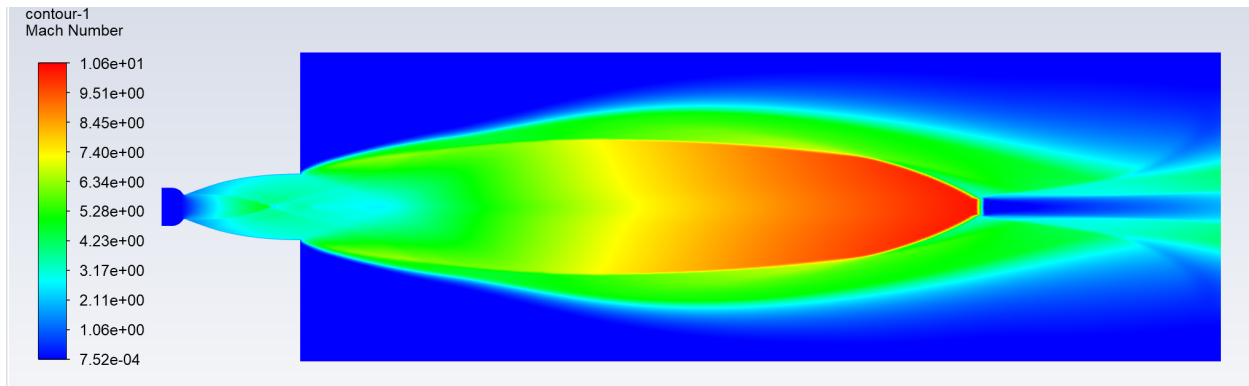


Figure 3.32 - Mach number contour for $P_0 = 6,000$ Pa

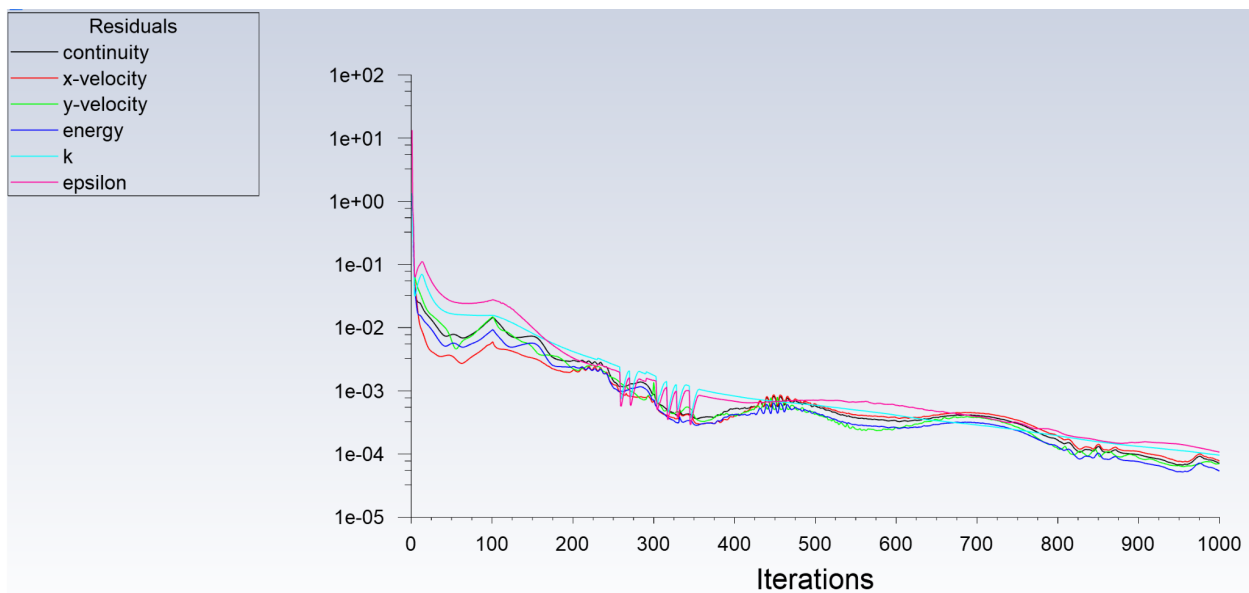


Figure 3.33 - Residuals for $P_0 = 6,000$ Pa

3.4 Propulsion Subsystem Conclusions

In conclusion, the CFD simulations show that the nozzle functions as expected with the design parameters developed in Section 3.2. Simulations were not possible at the near-vacuum conditions of the Martian atmosphere. However, a trend can be seen by simulating the nozzle in atmospheric pressures from 101,325 Pa (14.69 PSI) to 6,000 Pa (0.87 PSI). As expected, there are no oblique shock reflections within the nozzle at all altitudes due to the use of the method of characteristics for nozzle design. At sea-level conditions, the nozzle is slightly over expanded, with a perfectly expanded nozzle at about 40,000 Pa (5.8 PSI). At 6,000 Pa (0.87 PSI), there is an extremely underexpanded nozzle which is to be expected at near vacuum environments. From this data, it can be extrapolated that the nozzle will also be free of oblique shock reflections within the Martian atmosphere. The thrust capability of this engine in all altitudes of the Martian atmosphere is theoretically calculated to be 2.42 MN (0.544×10^6 lbf).

The design and simulation of the nozzle can be improved with more advanced CFD software that is more capable of simulation within a vacuum. To reflect the area ratios of vacuum

engines more accurately, a higher area ratio of greater than 40 can be used. However, a minimum length nozzle would not be feasible due to the extreme lengths at high area ratios. Therefore, a parametric study of various divergent contours of shorter lengths is needed to ensure no shocks are reflected within the nozzle.

Chapter 4: Orbital Dynamics

Orbital trajectories are critical for an efficient mission to Mars. An orbital trajectory for the Mars Landing System was designed by studying historical data of orbits and trajectories of past missions to Mars. Orbital dynamics theory was used to design the various mission phases by leveraging trends in historical data. Critical characteristics of the orbital trajectory were then simulated using NASA’s GMAT.

4.1 Historical Data and Analysis

There were many successful missions to Mars from multiple nations. These missions include orbiters, landers, rovers, and now rotorcraft. The United States has flown the greatest number of successful missions to Mars. Therefore, the historical data analysis will focus on recent missions planned by the United States. Table 8 summarizes the masses of various spacecraft, launch site, launch vehicles used, and any trajectory details readily available.

Table 4.1 - Historical mars mission data [27]

Mission	Mass	Launch Site	Launch Vehicle	Trajectory Details
Perseverance	1,025 kg	KSC	Atlas V 541	Up to 6 Trajectory Correction Maneuvers
InSight	360 kg	Vandenberg	Atlas V 401	Up to 6 TCMS
Maven	2454 kg	KSC	Atlas V 401	Hyperbolic earth orbit at 196 x 78,200 km hyperbolic at 27.7 degree inclination, trans mars trajectory, then martian orbit.
Curiosity	3,893 kg	KSC	Atlas V 541	Up to 5 Trajectory Correction Maneuvers
Phoenix	664 kg	KSC	Delta 7925-9.5	165 x 324 km around earth 35.5 inclination.

Mission	Mass	Launch Site	Launch Vehicle	Trajectory Details
Mars Reconnaissance Orbiter	2180 kg	KSC	Atlas V 401	Earth orbit, Mars intercept, highly elliptical orbit 426 x 44,500 km, aerobreaking and TCMs to 250 x 316 km orbit
Spirit/Opportunity	1062 kg	KSC	Delta 7925-9.5	Parking orbit at 28.5 deg inclination > heliocentric orbit, 3 corrections

The historical data shows there were no missions to Mars with spacecraft at the scale required for human spaceflight. However, the total mass is not critical for calculating orbital trajectories. Most of the recent spacecraft launched from NASA's Kennedy Space Center in Florida, with only one launching from Vandenberg Space Force Base in California [27]. The launch vehicles used were Boeing's Delta 7925 and United Launch Alliance's Atlas V [27]. Both do not have the ΔV capabilities for human spaceflight to Mars. Each spacecraft varied in the number of Trajectory Correction Maneuvers, TCMs, with a maximum of 6 [27]. Parking orbit inclinations ranged from 27.7 degrees to 35.5 degrees [27].

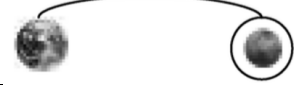
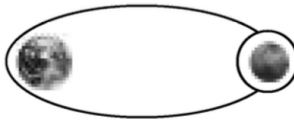
The historical data shows a trend that 6 TCMs are an ideal quantity. The parking orbit inclinations are primarily limited by Kennedy Space Center's range restrictions [28]. These restrictions prevent any flight path over populated land masses [28]. Therefore, a tentative parking orbit inclination of 27.7 degrees will be selected. Lower inclinations allow launch vehicles to take advantage of rotation of the Earth which leads to less ΔV expenditure at launch. This is desirable to allow for larger spacecraft masses.

4.2 Theory

Orbital trajectory theory is well established and has not significantly changed since the first missions to space. In this section, ΔV s for a Hohman transfer to Mars will be calculated. Additionally, important aspects such as mission duration will also be covered.

There are multiple types of Mars trajectories. The different types are discussed in Chapter 1 of this report and summarized in Table 4.2 [11]. The semidirect trajectory is ideal for the MLS because it allows for a direct transit to Mars orbit which minimizes travel time. The benefit for this is twofold; the spacecraft crew will spend less time in a dangerous space environment, and the crew will get more time on Mars.

Table 4.2 - Trajectory types between Earth and Mars [11].

Architecture	Earth Encounter	Mars Encounter	Schemata
Direct	Surface	Surface	
Semidirect	Surface	Parking orbit	
Stopover	Parking orbit	Parking orbit	
M-E semicycler	Flyby	Parking orbit	
E-M semicycler	Parking orbit	Flyby	
Cycler	Flyby	Flyby	

The synodic period between celestial bodies is the time it takes for both bodies to return to a specific position relative to each other when orbiting the Sun [16]. This concept is critical for selecting the most energy-efficient launch window between Earth and Mars. Earth and Mars do not have equal orbital periods, so the synodic period is defined by Eq. (4.1), where T_{EARTH} is the orbital period of Earth at 365.26 days and T_{MARS} is the orbital period of Mars at 687.99 days [16].

$$T_{SYNODIC} = \frac{T_{EARTH} * T_{MARS}}{|T_{EARTH} - T_{MARS}|} = 778.65 \text{ days} \quad (4.1)$$

Historical launch data can be used as a baseline to determine future launch windows by adding 778.65 days to the launch windows of previously successful flights [16]. Most recently, three launches left for Mars in July 2020, meaning a rough target for a future launch date can be written as:

$$T_{LAUNCH} = T_{HISTORICAL} + n * T_{SYNODIC} \quad (4.2)$$

Table 4.3 - Launch opportunities

Launch Opportunities Number	Date
1	August 2022
2	October 2024
3	November 2026
4	January 2029
5	February 2031
6	April 2033

After determining when the launch can happen, the next step is to determine how it will happen. Figure 36 is a diagram of an interplanetary trajectory that utilizes a Hohmann transfer to transit from one planet to another [16]. Hohmann transfers are ideal for interplanetary travel since these transfers require the least amount of energy expenditure [16].

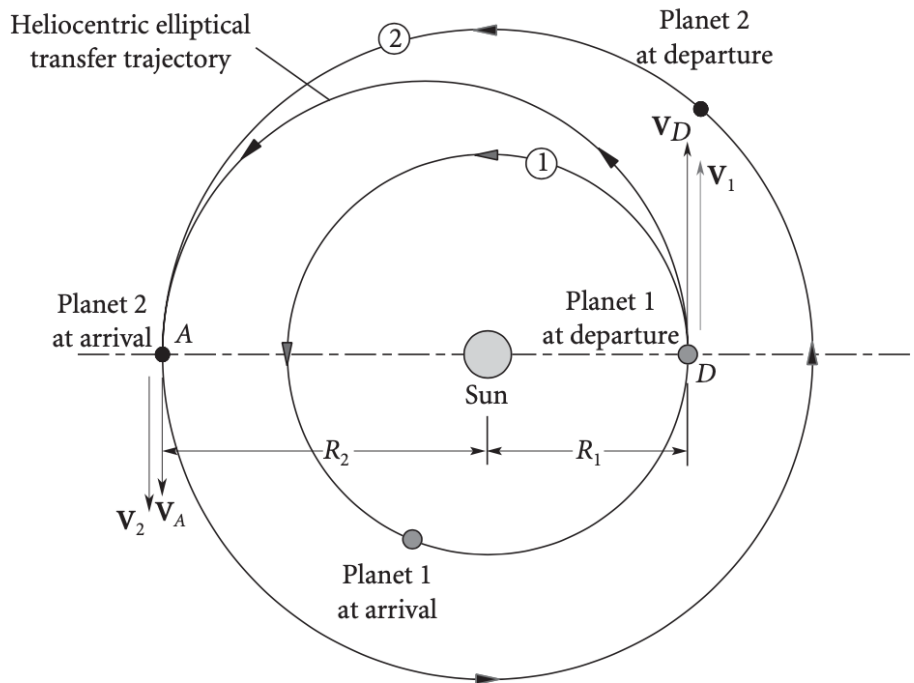


Figure 4.1 - Hohmann transfer diagram [16].

The most critical aspect is determining the change in velocity required to depart the gravity of Earth and the change in velocity required to safely arrive on Mars. This parameter is ΔV which can be divided into $\Delta V_{DEPARTURE}$ and $\Delta V_{ARRIVAL}$, and both are calculated with the following

equations. Although the orbits of Earth and Mars are at slightly different inclinations and are elliptic, the following equations assume coplanar, and circular orbits for a rough estimate. The orbital radius of Earth, R_{EARTH} is 1.496×10^{11} m. The orbital radius of Mars, R_{MARS} is 2.279×10^{11} m. The standard gravitational parameter of the Sun, μ_{SUN} is $1.327 \times 10^{20} \text{ m}^3\text{s}^{-2}$ [16].

$$\Delta V_{DEPARTURE} = \sqrt{\frac{\mu_{SUN}}{R_{EARTH}}} \left(\sqrt{\frac{2R_{MARS}}{R_{EARTH} + R_{MARS}}} - 1 \right) \quad (4.3)$$

$$\Delta V_{ARRIVAL} = \sqrt{\frac{\mu_{SUN}}{R_{MARS}}} \left(1 - \sqrt{\frac{2R_{EARTH}}{R_{MARS} + R_{EARTH}}} \right) \quad (4.4)$$

Eqs. (4.3) and (4.4) lead us to a $\Delta V_{DEPARTURE}$ and $\Delta V_{ARRIVAL}$ of 2.94×10^3 m/s and 2.65×10^3 m/s respectively for a total ΔV of 5.59×10^3 m/s (18.34×10^3 ft/s) [16]. The travel time from Earth to Mars is given by the following equation. This represents the maximum travel time, utilizing the smallest ΔV .

$$T_{TRANSIT} = \frac{\pi}{\sqrt{\mu_{SUN}}} \left(\frac{R_{EARTH} + R_{MARS}}{2} \right)^{3/2} \quad (4.5)$$

Eq. (4.5) yields 258.8 days for the transit time from Earth to Mars as well as the time it takes to return from Mars to Earth. Although the travel time is the same for outgoing and return trips to Earth, the most efficient time to travel from Earth to Mars is not the same time period for the most efficient return trip from Mars to Earth [16]. The following Eq. (4.6) is used to calculate the most effective time period for a mission on the Martian surface [16]. Since the most efficient return launch window is a recurring time period, $n = 1$, represents the first opportunity for an efficient return, $n = 2$, represents the second opportunity, and so forth.

$$T_{SURFACE} = \frac{-2 * \left(\pi - \frac{2\pi}{T_{EARTH}} \frac{\pi}{\sqrt{\mu_{SUN}}} \left(\frac{R_{EARTH} + R_{MARS}}{2} \right)^{3/2} \right) - 2\pi n}{\frac{2\pi}{T_{MARS}} - \frac{2\pi}{T_{EARTH}}} \quad (4.6)$$

Table 4.4 - Mission durations

Return Opportunity Number	Surface Mission Duration	Total Mission Duration
1	453.8 days	971.4 days
2	1232.4 days	1750.1 days
3	2011.1 days	2528.7 days
4	2789.8 days	3307.4 days
5	3568.4 days	4086.0 days

To leave the Martian surface, the ΔV requirement is the same as the ΔV needed to leave Martian orbit, $\Delta V_{ARRIVAL}$. This is 2.65×10^3 m/s (8.69×10^3 ft/s).

4.3 Simulation

NASA's General Mission Analysis Tool (GMAT) is used to simulate the interplanetary Hohmann transfer trajectory from Earth to Mars. The previously calculated mission durations, and ΔV s are used as inputs. The following simulation is of a semi-direct mission architecture with a launch from Earth to Martian Orbit Insertion. The Mavem spacecraft followed this trajectory. Therefore, the Mars Landing System, MLS, mission is simulated using the exact launch date and time of the Mavem spacecraft. GMAT parameters such as spacecraft mass and fuel are updated to reflect MLS and Falcon Heavy performance attributes. Future launch periods can be determined by adding the synodic period to the launch time.

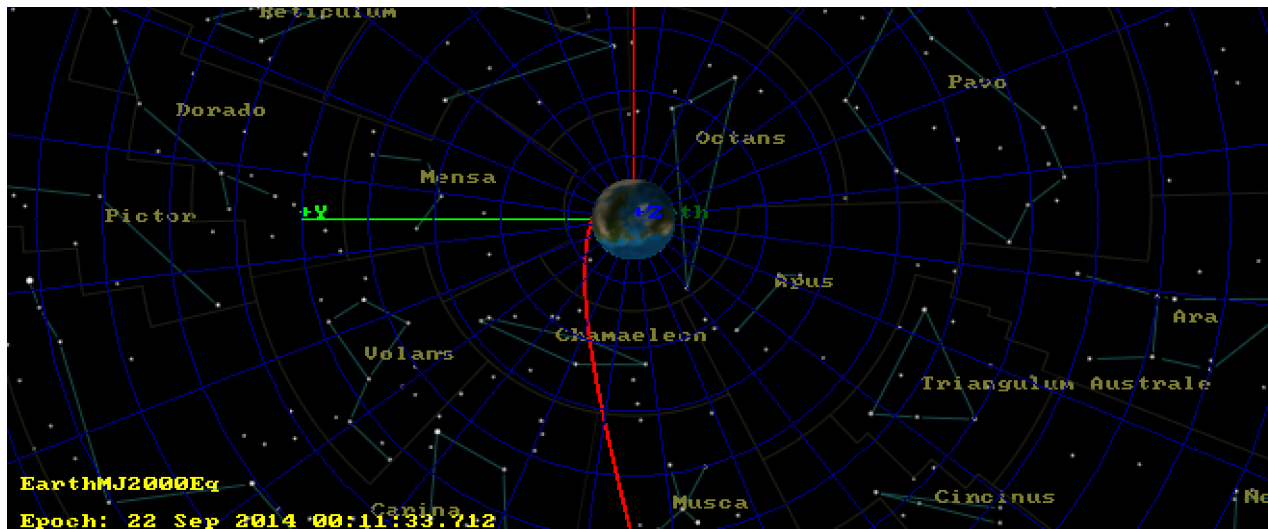


Figure 4.2 - Earth departure

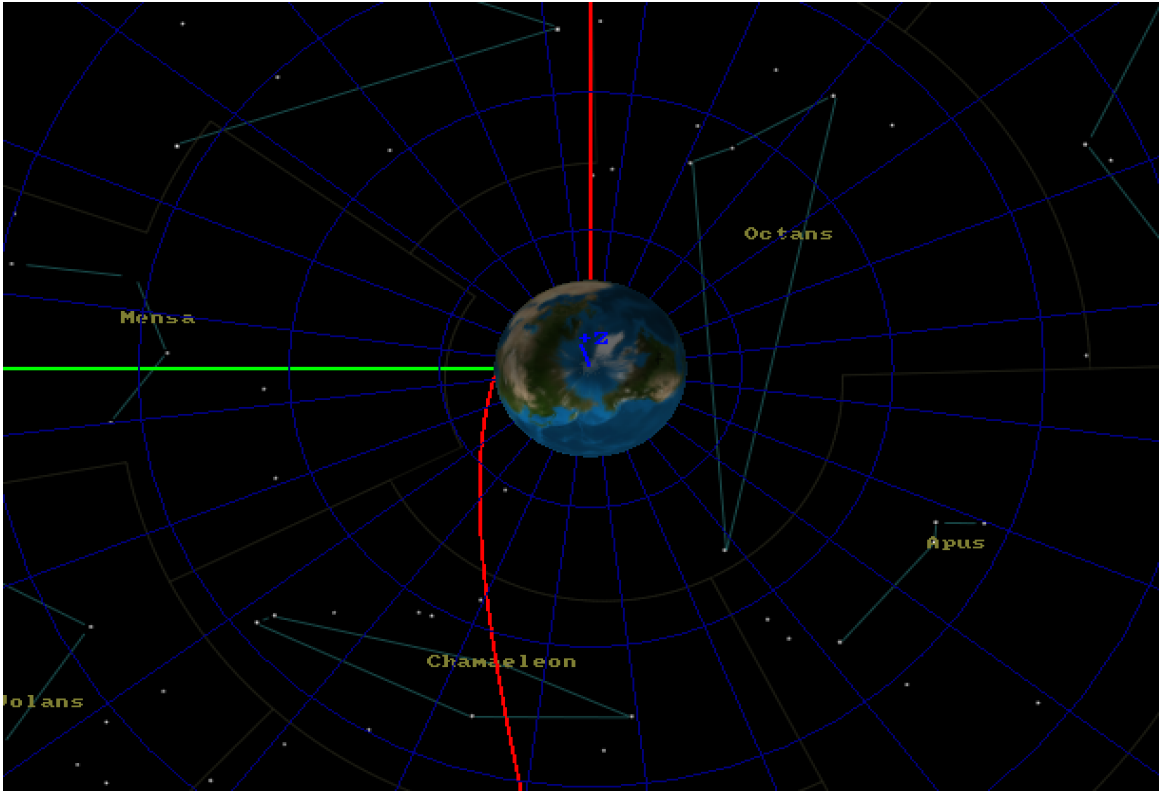


Figure 4.3 - Earth departure closeup

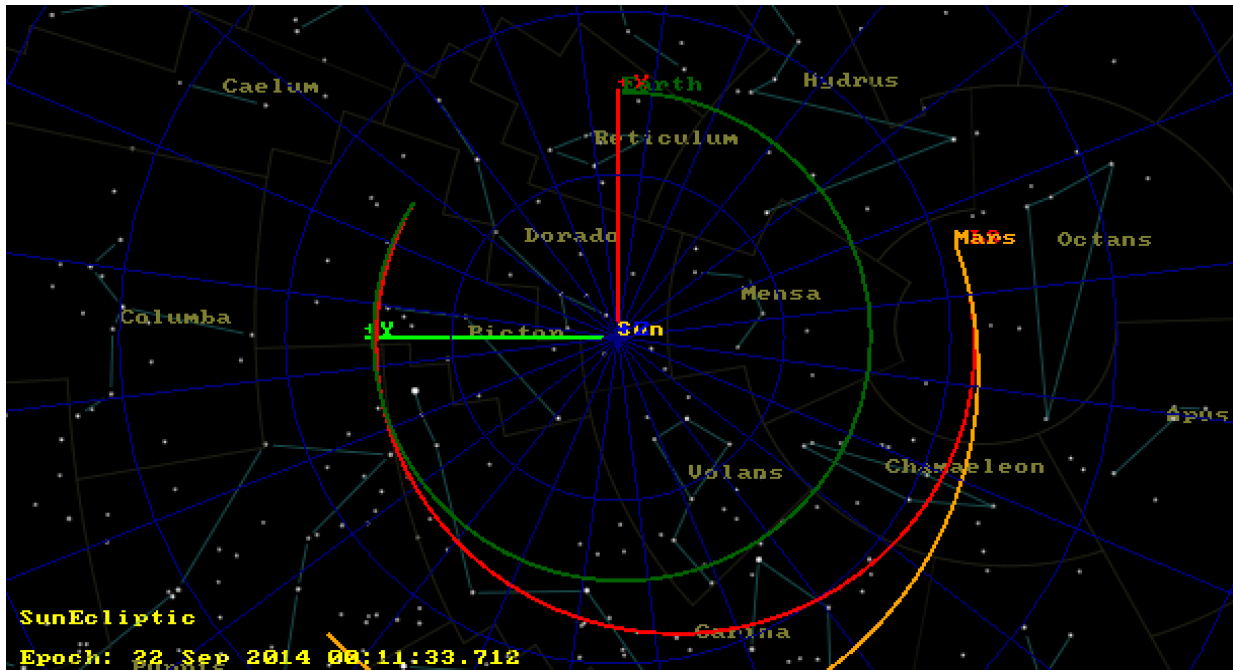


Figure 4.4 - Hohmann transfer trajectory

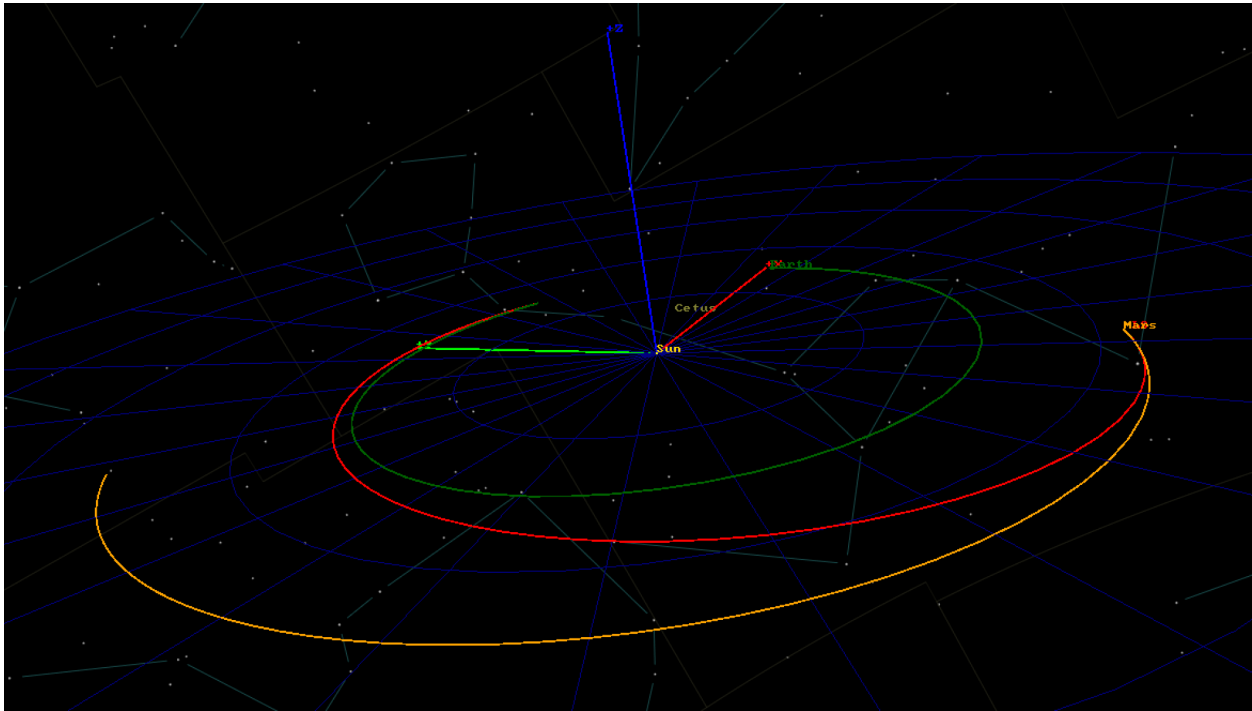


Figure 4.5 - Hohmann transfer isometric view

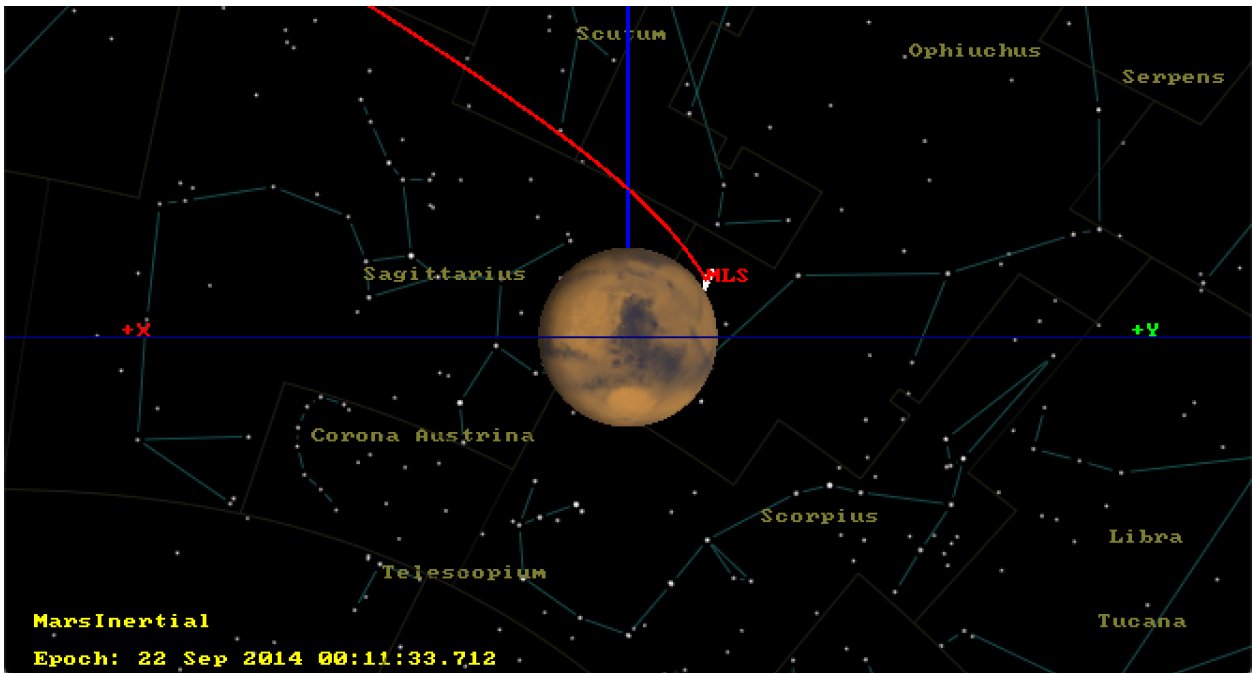


Figure 4.6 - Mars orbit insertion

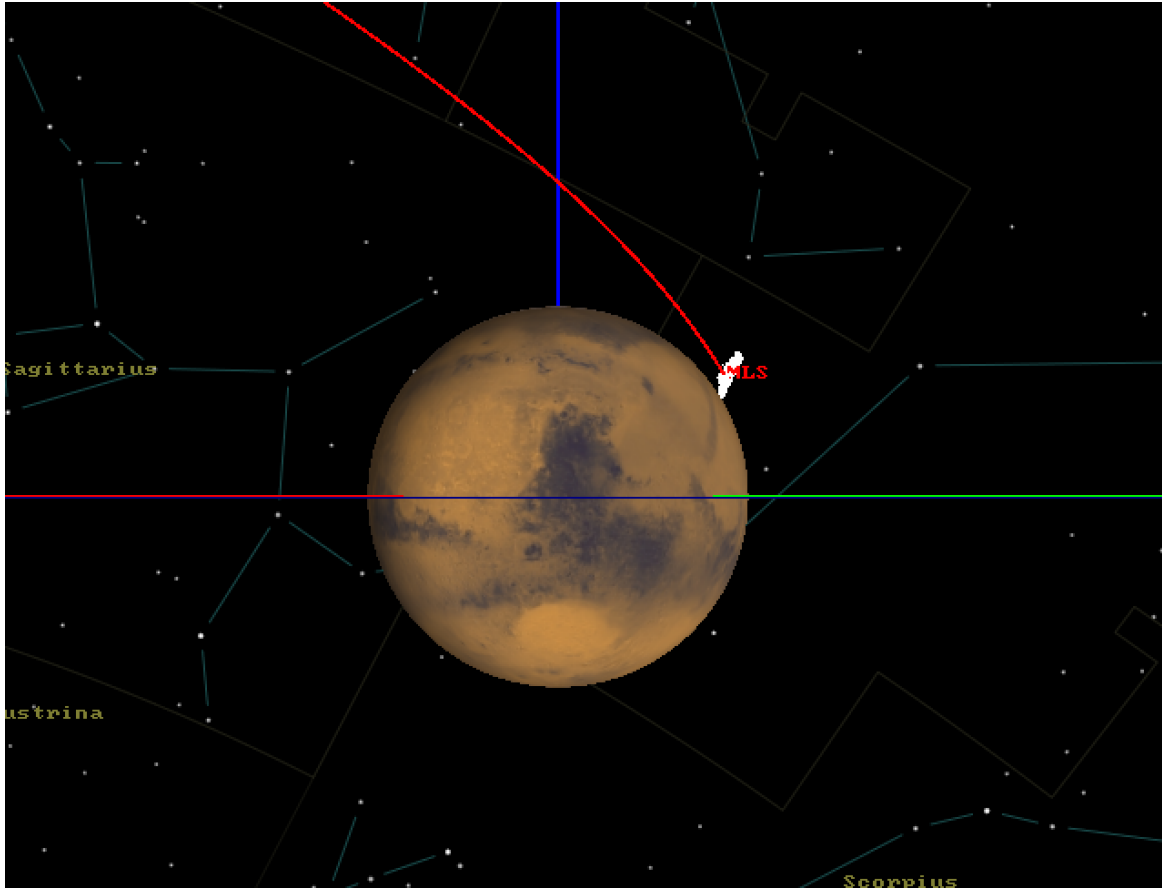


Figure 4.7 - Mars orbit insertion closeup

Using similar methods, the return trip to Mars can also be simulated. A departure from Martian orbit directly to the surface of Earth. Since the mission duration from Mars to Earth takes the same amount of time, with the same ΔV s, the return trip is essentially an inverted outgoing trip, as shown in the following figures.

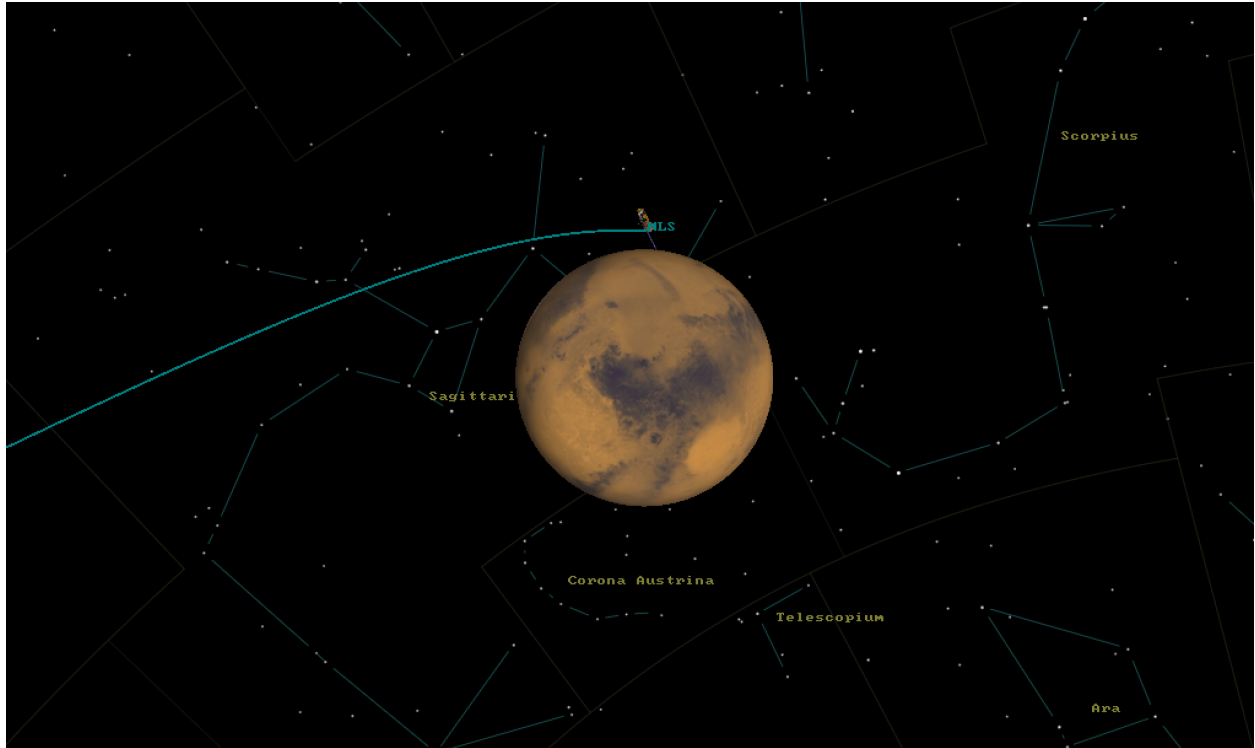


Figure 4.8 - Mars orbit departure

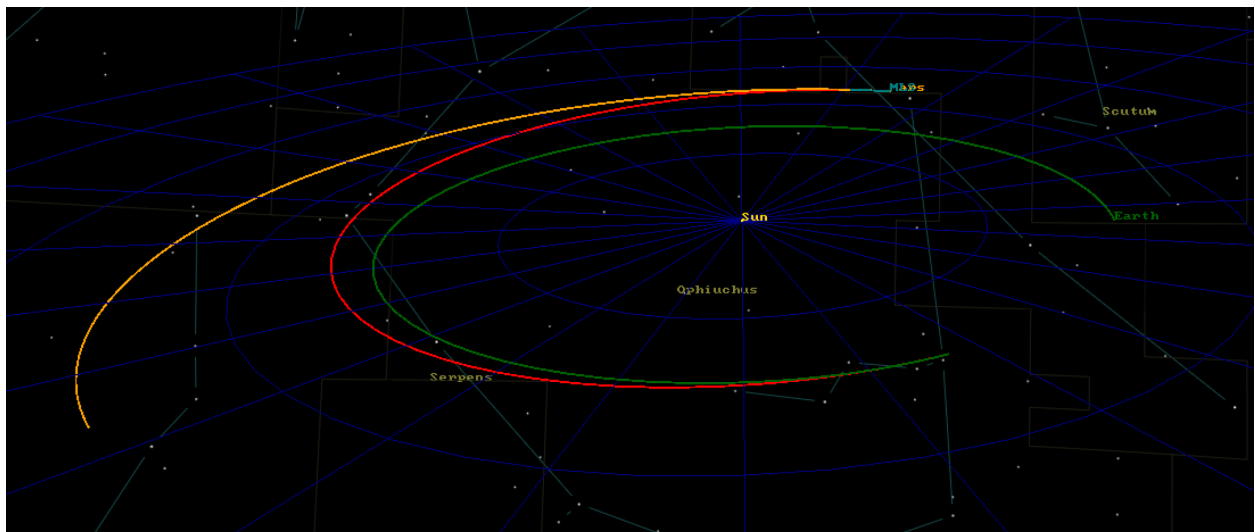


Figure 4.9 - Mars to Earth orbital trajectory

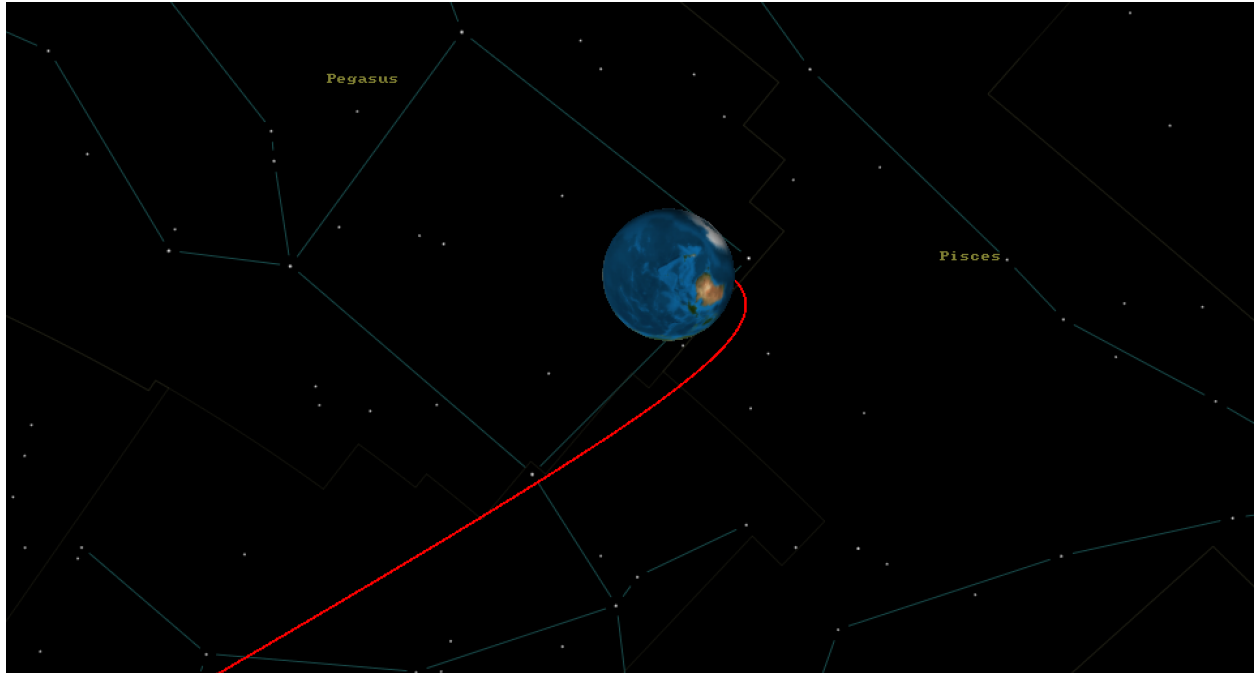


Figure 4.10 - Earth arrival

4.4 Conclusions

The MLS will launch from Kennedy Space Center, Florida with an initial inclination of 27.7 degrees to comply with launch complex safety requirements while still taking advantage of Earth's rotation for a ΔV boost. The spacecraft will then follow an interplanetary Hohmann transfer orbit to Mars orbit with a ΔV of 2.94×10^3 m/s (9.65×10^3 ft/s). The trip to and from Mars is expected to take 258.8 days with a total mission duration of 971.4 days or 2.7 years. However, if the initial return launch window is missed, the mission can be extended to 1750.1 days or 4.8 years.

Chapter 5: Program and Mission Planning

This chapter will cover program and mission planning at a high level. The following sections will cover:

- How and when the Mars Landing System will be developed
- What each component does
- How each component is used
- What the potential benefits of a Martian mission are

5.1 Project Development

The development of the MLS is a large and ambitious program. Therefore, it is beneficial to break up the program into milestones. Milestones are broken up into four categories:

- Earth-Based Testing
- Low-Earth Orbit Based Testing
- Mars-Based Testing
- Production Line Qualification

5.1.1 Earth-based Testing Milestones

Earth based testing will be conducted at the component, subsystem, and system levels. The milestones for each subsystem can be completed in parallel to reduce the schedule and provide additional slack for unforeseen issues.

The fuel production system will be tested in a simulated Mars atmosphere on Earth. A proof-of-concept test article would be constructed and tested first. The purpose of the first test article is to simply prove that the subsystem can create fuel and can be made from consumer off the shelf, COTS, hardware. The next milestone is to construct and test a spaceflight-qualified fuel production system.

The propulsion subsystem will have three major milestones. The first will be the construction and test of a scaled test article. The goal of this test is to confirm mixing ratios and nozzle geometry performance. The second milestone is the testing of the full-scale propulsion system. The third test will be a system-level test of the propulsion system integrated into the ascent and descent modules.

Similar to the propulsion system, the reentry system will also be tested at scale. Hypersonic wind tunnels will be used. Then another scaled model will be tested reentering the atmosphere of Earth. For this test, the upper atmospheric data will be most critical as the less dense upper atmosphere is most similar to the Martian atmosphere in terms of density. Finally, a full-scale test will be tested reentering the upper atmosphere.

The major milestones for the structure of the spacecraft will be structural proof testing. These tests will confirm that the structure of each module can withstand the loads of repeated launches and reentries. The crew module will also be pressure tested.

The life support milestone is the testing of all systems required to ensure crew survivability. This includes systems to maintain an Earth-like atmosphere with the appropriate oxygen and carbon dioxide levels and temperature control. Water recycling and sanitation systems will also be tested.

A multi-purpose rover will also need to be tested. This rover will serve as transport for the fuel module as well as transport for the crew for surface activities. The rover will also be used to help in the construction of a Martian base.

The following table summarizes the Earth-based milestones for the development of the MLS.

Table 5.1 - Earth-based milestones

Milestone	Subsystem	Description
Fuel Module Proof of Concept	Fuel Module	Successful test of fuel production system.
Fuel Module Spaceflight Qualification	Fuel Module	Successful qualification for spaceflight of fuel production system.
Scaled Propulsion Test	Propulsion	Successful confirmation of fuel ratio and nozzle geometry performance.
Full Scale Propulsion Test	Propulsion	Successful land based test of spaceflight hardware.
MLS Module Test Launch	Propulsion/Structural	Successful test launch of ascent and descent modules.
Hypersonic Wind Tunnel Heat Shield Testing	EDL	Successful confirmation of heat shield performance characteristics
Scaled Atmospheric Reentry Test	EDL	Successful test of deployable heat shield technology.
Full Scale Atmospheric Reentry Test	EDL/Structural/Propulsion	Successful test of full scale spaceflight hardware.
Structural Testing	Structural	Successful confirmation that spacecraft structure and withstand static, dynamic, and vibrational loads.
Crew Module Pressure Testing	Structural	Successful cyclical pressurization of the crew module.

Milestone	Subsystem	Description
Life Support Testing	Life Support	Successful testing of atmospheric, water, and sanitation systems.
Rover Qualification	Fuel Module	Successful test of fuel module rover systems.

5.1.2 Low-Earth Orbit-Based Testing Milestones

Low-Earth orbit-based testing will be conducted once all Earth-based testing is completed successfully.

Production models of each module will be launched into low-Earth orbit, LEO. Testing will then be conducted to test the GNC capabilities of each module and their ability to dock with each other and to the ISS. Orbital refueling will also be tested at the point.

A shakeout test of procedures needed for Mars exploration will take place. These include crew and cargo loading, docking and undocking procedures.

The following table is a summary of the LEO-based testing milestones.

Table 5.2 - Low earth orbit milestones

Milestone	Subsystem	Description
MLS LEO Test	GNC, Life Support, Structural	Successful launch, assembly, checkouts, and docking in space.
MLS LEO Procedure Shakeout	All	Successful tests of system level procedures needed for Mars exploration.

5.1.3 Mars-Based Testing Milestones

A cubesat will be launched to Mars following the planned trajectory for MLS modules. This will serve as a pathfinder to prove the calculated orbital trajectories are sound.

System-level Mars-based testing will be conducted once all LEO milestones are successfully achieved. An uncrewed crew module and a cargo module with ballast weight will land on Mars. A second system-level test will be the launch of the modules back into orbit.

The following table is a summary of Mars based testing milestones.

Table 5.3 - Mars based testing milestones

Milestone	Subsystem	Description
Cubesat Trajectory Test	GNC	Successful test flight of the orbital trajectory utilizing a cubesat.
MLS Mars Landing	All	Successful uncrewed landing on Mars.
MLS Mars Launch	All	Successful uncrewed launch from Mars.

5.1.4 Production Line Qualification Milestones

Following the successful testing of all development milestones, the program then shifts into production mode. Multiple MLS modules will be needed. Therefore, a production line will need to be developed. Ideally, each module will be designed with sustainability and manufacturability in mind. The health and safety of the production line employees will also be considered. To save time, the production line will be in development at the same time the production hardware is being designed.

Table 5.4 - Production line milestones

Milestone	Subsystem	Description
Production Line Qualification	Production	Successfully develop a production line that can sustainably manufacture the required number of MLS modules without sacrificing health and safety of employees.

5.1.5 Schedule

The following figure is the estimated schedule for the MLS program through research and development, to the return of the first crew from Mars.

5.2 Module Descriptions and Concept of Operations

The Mars Landing System, MLS, consists of a crew module, cargo module, descent module, and refueling module. For the MLS to support a crewed mission to Mars, additional hardware is required. This includes crewed rovers, a Martian space station, cargo pods, and an interplanetary transit vehicle.

The crew module consists of inhabitable space for four astronauts. It utilizes two rocket engines that were designed in Chapter 3 and also has a reaction control system, RCS. The crew module also serves as a lifeboat for the astronauts and contains all necessary life support systems.

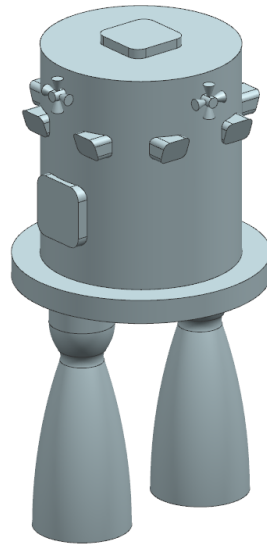


Figure 5.1 - Crew module

The cargo module is similar to the crew module in terms of propulsion and RCS systems. The primary difference is that the cargo module has larger fuel tanks. The cargo modules serve a secondary purpose as orbital refueling tankers. The cargo modules also have a flat area for mounting cargo pods instead of a pressurized crew cabin.

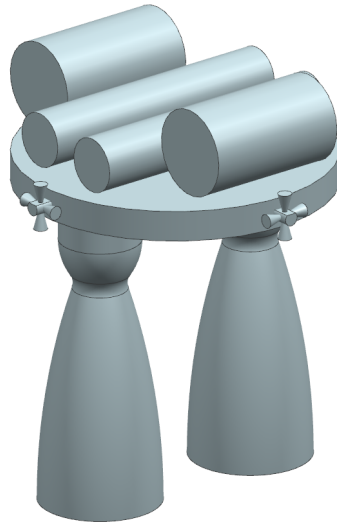


Figure 5.2 - Cargo module

The descent module is based on the cargo module. Instead of larger fuel tanks, the descent module has a reusable deployable heat shield. The descent module also has single stage to orbit capabilities, but it does not have a robust GNC or RCS system. To return to the space station for refueling, either the crew or cargo modules will dock with the descent module once in orbit.

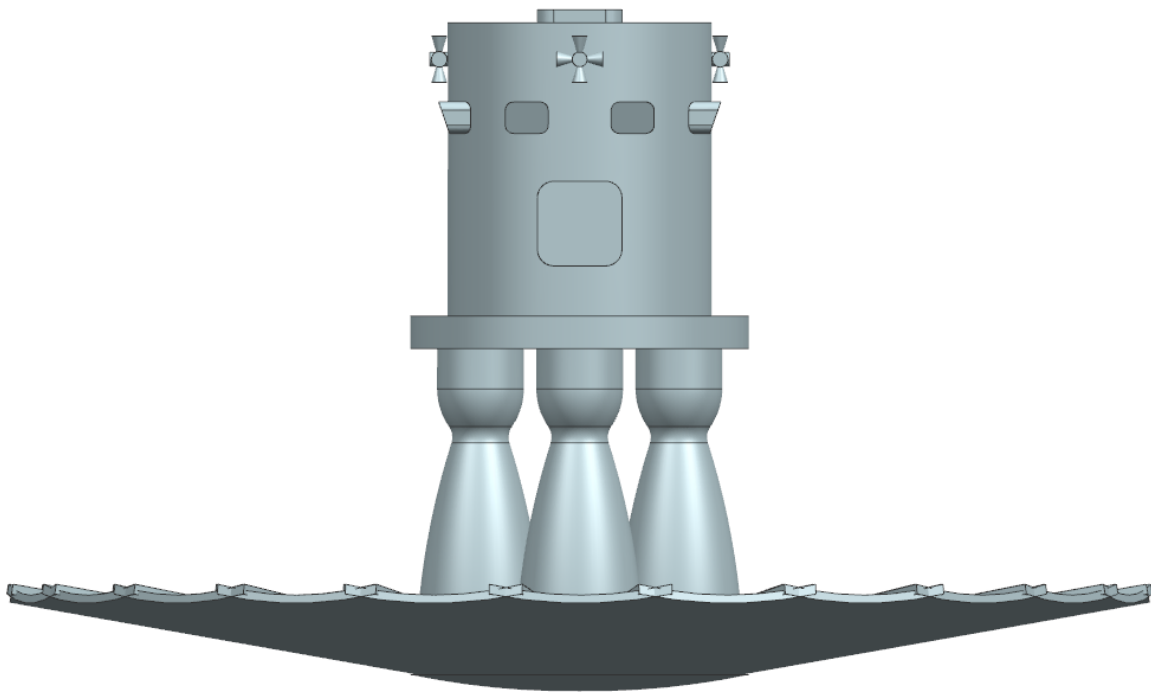


Figure 5.3 - Descent module with crew module

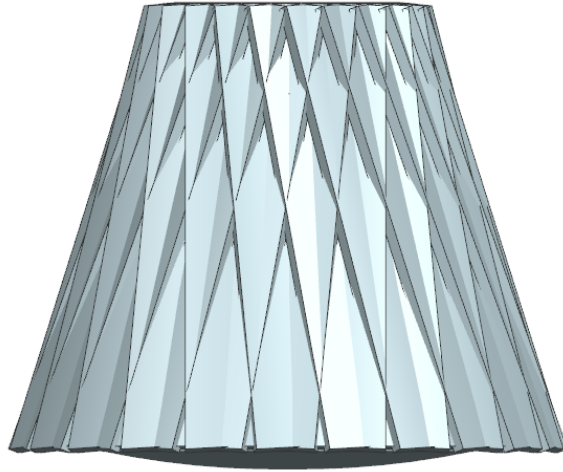


Figure 5.4 - Descent module with folded heat shield to return to orbit

The refueling module is a static fixture that produces fuel from the Martian atmosphere. The refueling module will be attached to a rover, and this assembly is brought to the surface via the cargo module.

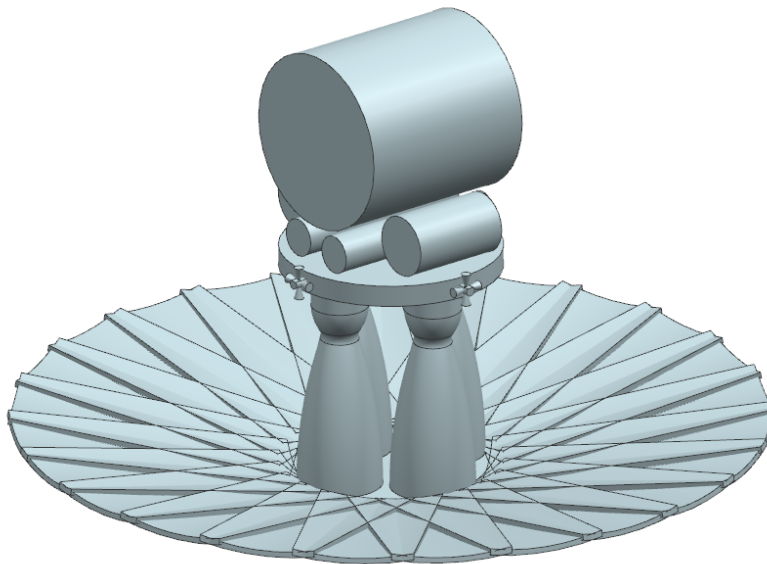


Figure 5.5 - Descent module with cargo module and fuel module

A transit module, cargo pods, and an interplanetary transit vehicle are outside the scope of the lander design program, but requirements are described in this paragraph. A transit module is required for the nearly year-long journey between Earth and Mars. The transit module should have private sleeping quarters for each crew, a restroom, a gym, and life support. The Orion capsule would remain docked to the transit module while traveling between Earth and Mars. A Martian

Space Station with refueling tanks would be required to store excess fuel from the cargo modules. Cargo pods will also need to be designed that could also double as inhabitable modules for a space base. A rover with a construction crane would also be beneficial for building a Martian base.

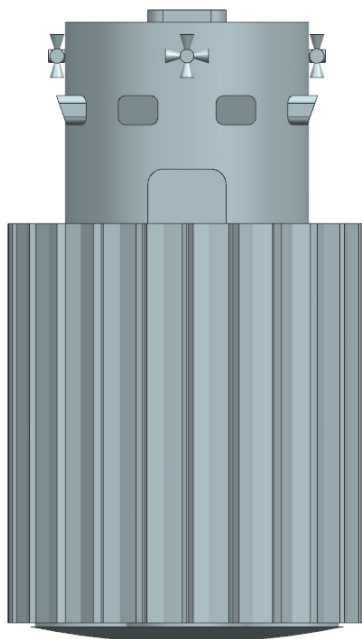


Figure 5.6 - Descent module with crew module in transit configuration

5.3 Mission Operations

This section will describe the mission operations for the first crewed mission to Mars using the Mars Landing System, MLS.

Uncrewed hardware will launch to Mars in 2031. This includes 1 crew module, 1 refueling module, 7 cargo modules, and 8 descent modules. Along with the MLS modules, cargo pods with enough consumables for 2000 days will be sent to Mars. This is enough consumables to support human life for 250 days beyond the second return opportunity. A single cargo and descent module will land first to ensure all systems are working properly. Then the remaining 7 landers will target reentry in the same area. Due to the high number of modules, multiple launches will be required. The modules can be placed in a parking orbit in LEO until the best transit opportunity to Mars arrives.

Rovers that landed with the cargo modules will begin bringing the cargo pods to an ideal base location while the refueling module begins to create fuel from the atmosphere.

The return to orbit functionality of the crew module will be tested as it launches from the Martian surface to dock with the Martian space station. The remaining crew and cargo modules will be refueled and also return to the space station.

In 2033 the crew will launch with any additional cargo. Once the crew reaches the Martian space station, the crew will board the crew and descent module combo and travel down to Mars' surface. Once the crew lands, the rovers will travel to the landing site to pick them up and take them to the planned base location so the crew can begin assembling the base.

The remaining cargo and descent modules that are still at the space station will begin bringing down additional cargo that would be used during follow-on crewed missions.

After 453.8 days on Mars' surface, the crew will begin their journey back to Earth and will splash down in another 258.8 days.

5.4 Program Benefits

The Mars Landing System, MLS, program has immediate benefits for the scientific and engineering communities. It will expand the scientific community's knowledge of the universe and its formation, as well as advance technology used in exploring the solar system.

Beyond the immediate scientific and technological benefits, there are also:

- Ethical benefits
- Political benefits
- Societal benefits
- Economic benefits
- Environmental benefits

Space funding could be diverted to many other social programs that would provide a greater immediate benefit to society such as:

- Fighting poverty
- Funding education
- Preventing disease

However, funding a space program is still an ethical choice because of the long-term benefits it could provide.

The first ethical benefit is that civilian space programs keep engineers out of the weapons industry. If funding for civilian space were suddenly cut, there would be thousands of unemployed engineers who could easily repurpose their skill sets to make weapons of war [29]. Space programs also foster international cooperation among adversaries such as the United States and Russia cooperating to build the International Space Station [29]. This cooperation is a political benefit that can be one of many reasons that would help prevent the outbreak of war.

Space programs have been increasingly more democratic by being more representative of the United States' demography. The Apollo program started with only white males going to space. However, starting with the Space Shuttle, the public started to see women and people of color in space [30]. Then with the International Space Station, the LGBT community and international partners saw more representation in space [30]. The upcoming Artemis missions also plan to send the first woman and first man of color to the Moon.

The environmental and economic benefits are also significant for a Mars mission. Conducting science on the surface of Mars will help scientists better understand what happened to the water and atmosphere on Mars. This could impact how people protect the natural resources of Earth [31]. A program of this scale also means thousands of good-paying jobs with most of the manufacturing jobs being union jobs [32].

References

- [1] Connolly, J. F., “After LM, NASA Lunar Lander Concepts Beyond Apollo,” NASA SP-2020-220338, NASA JSC-E-DAA-TN69151, October 2019.
- [2] Polsgrove, T., Thomas, D., Sutherlin, S., Stephens, W., and Rucker, M., “Mars Ascent Vehicle Design for Human Exploration,” NASA M16-5281, August 2015.
- [3] Polsgrove, T., Fabisinski, L., Collins, T., Cianciolo A.D., Samereh, J., Robertson, E., Studak, B., Vitalpur, S., and Lee, A.Y., “Human Mars Lander Design for NASA’s Evolvable Mars Campaign,” NASA M16-5076, March 2016
- [4] Craig, A.S., Holt, J.P., Hannan, M.R., and Orphee, J.I., “Mission Design for the Lunar Pallet Lander,” NASA M18-7143-1, American Astronautical Society Paper 19-330, January 2019.
- [5] Sforza, P.M., “Spacecraft Configuration Design,” *Manned Spacecraft Design Principles*, 1st ed., Vol. 1, Elsevier Butterworth-Heinemann, Massachusetts, 2015, pp. 542-556.
- [6] Story, G.T., Karp, A.C., Nakazona, B., Whittinghill, G., and Zilliac, G.G., “Mars Ascent Vehicle Hybrid Propulsion Development,” NASA M19-7375, June 2019.
- [7] MacKay, J.S., Zola, C. L, Rossa, L.G., Fishbach, L.H., Strack, W.C., and Hrach, F.J., “Manned Mars Landing Missions using Electric Propulsion,” NASA TN-D-3194, January 1966.
- [8] Percy, T., Polsgrove, T., and Thomas, D., “Methane Propulsion Elements for Mars,” NASA M17-5956, April 2017.
- [9] Yaghoubi, D., and Schnell, A., “Mars Ascent Vehicle Solid Propulsion Configuration,” NASA M19-7660, March 2020.
- [10] Turner, M.J., “Liquid Propellant Rocket engines” *Spacecraft Propulsion Principles, Practice and New Developments*, 3rd ed. New York, November 2009, pp. 133-141.
- [11] Landau, D.F., Longuski, J.M., “Trajectories for Human Missions to Mars, Part 1: Impulsive Transfers,” *Journal of Spacecraft and Rockets*, Vol. 43, No. 5, pp. 1035-1042. <https://doi.org/10.2514/1.18995>
- [12] Burke, L. “An Examination of ‘The Martian’ Trajectory,” NASA GRC-E-DAA-TN27094, October 2015.
- [13] Chai, P. R., Merrill, R. G., and Qu, M., “Mars Hybrid Propulsion System Trajectory Analysis Part I: Crew Missions,” NASA NF1676L-20722, VA, August 2015.
- [14] Abilleira, F., “2011 Mars Science Laboratory Trajectory Reconstruction and Performance from Launch through Landing,” American Astronautical Society Paper 04-113, February 2013.
- [15] Curtis, H. D., “Interplanetary Trajectories,” *Orbital Mechanics for Engineering Students*, 1st ed., Elsevier Butterworth-Heinemann, Massachusetts, 2005, pp. 347-398.
- [16] Broyan J.L., Schlesinger, T., and Ewert, M.K., “Exploration Mission Benefits from Logistics Reduction Technologies,” NASA JSC-CN-35577, International Conference on Environmental Systems, 2016-140, July 2016.
- [17] Neeley, J.R., Jones, J.V., Watson, M.D., Bramon, C.J., and Inman, S.K., “NASA Space Rocket Logistics Challenges,” NASA M14-3517, May 2014.
- [18] Lopez, P., Schultz, E., Mattfeld, B., Stromgren, C., and Goodliff, K., “Logistics Needs for Potential Deep Space Mission Scenarios Post Asteroid Redirect Crewed Mission,” NASA JSC-CN-32967, March 2015.

- [19] Jones H.W., “Comments on the MIT Assessment of the Mars One Plan,” NASA ARC-E-DAA-TN24213, International Conference on Environmental Systems, 2015-044, July 2015.
- [20] Larson, W.J., Wertz, J.R., “Mission Operations,” *Space Mission Analysis and Design*, 3rd ed. Microcosm Press, California, 2005, pp. 587-616.
- [21] Haddox, E., “Vehicle Information,” NASA, retrieved July 1, 2021. <https://elvperf.ksc.nasa.gov/Pages/Vehicles.aspx>
- [22] Benson, T., “Specific Heat Capacity Calorically Imperfect Gas,” NASA, retrieved July 1, 2021. <https://www.grc.nasa.gov/www/BGH/realSpec.html>
- [23] Hall, N. “Rocket Thrust Summary,” NASA, retrieved July 1, 2021. <https://www.grc.nasa.gov/www/k-12/airplane/rktthsum.html>
- [24] Hall, N., “Prandtl-Meyer Angle,” NASA, retrieved July 1, 2021. <https://www.grc.nasa.gov/www/k-12/airplane/pranmyer.html>
- [25] Anderson, J.D., “Inviscid, Compressible Flow,” *Fundamentals of Aerodynamics*, 5th ed., McGraw-Hill Education, New York, 2010, pp. 513-707.
- [26] Maurya, S., “Minimum Length Nozzle Design using Method of Characteristics,” MATLAB Central File Exchange, retrieved July 1, 2021. <https://www.mathworks.com/matlabcentral/fileexchange/57098-minimum-length-nozzle-design-using-method-of-characteristics>
- [27] “Mars Exploration Program,” NASA, retrieved September 8, 2021. <https://mars.nasa.gov/mars-exploration/missions/>
- [28] Jason, D., “Of Inclinations and Azimuths,” The Planetary Society, retrieved September 8, 2021. <https://www.planetary.org/articles/3450>
- [29] “America’s Future in Civil Space,” National Research Council, retrieved October 7, 2021. <https://www.nap.edu/read/24921/chapter/1>
- [30] Duane, H. “Diversity: It’s What Will Drive Aerospace Forward, AIAA, retrieved October 7, 2021. <https://scitech.aiaa.org/Forum.aspx?id=26555>
- [31] “Why go to Mars?”, European Space Agency, retrieved October 7, 2021. https://www.esa.int/Science_Exploration/Human_and_Robotic_Exploration/Exploration/Why_go_to_Mars
- [32] “Aerospace Engineering Job Outlook in the United States and Abroad,” University of Central Florida, retrieved October 7, 2021. <https://www.ucf.edu/online/engineering/news/aerospace-engineering-job-outlook-in-the-united-states-and-abroad/>

Appendix A – Sample Hand Calculations

$$(3.1) \quad \gamma_{gas} = 1 + \frac{1.4 - 1}{1 + (1.4 - 1) \left[\left(\frac{5000/1.8}{2000} \right)^2 \frac{e^{5000/1.8/2000}}{(e^{5000/1.8/2000} - 1)^2} \right]} = 1.2644$$

$$(3.2) \quad \gamma = \frac{(3.2)1.4 + 1.32}{(3.2) + 1} = 1.38$$

$$(3.3) \quad \frac{A_e}{A^*} = \left(\frac{1.256 + 1}{2} \right)^{-\frac{1.256+1}{2(1.256-1)}} \frac{\left(1 + \frac{1.256-1}{2} 2.3^2 \right)^{\frac{1.256+1}{2(1.256-1)}}}{2.3} = 2.494$$

$$(3.4) \quad \frac{T_e}{T_t} = \left(1 + \frac{1.256 - 1}{2} 2.3^2 \right)^{-1} = 0.5956$$

$$(3.5) \quad \frac{P_e}{P_t} = \left(1 + \frac{1.256 - 1}{2} 2.3^2 \right)^{-\frac{1.256}{1.256-1}} = 0.0791$$

$$(3.6) \quad v_e = 2.3 \sqrt{(1.256)(321.32)(2084.53)} = 2110 m/s$$

$$(3.7) \quad F = (997.04)(2110) + (316000 - 400)1 = 2.42 \cdot 10^6 N$$

$$(3.8) \quad I_{sp} = \frac{2.42 \cdot 10^6}{(997.04)(9.8)} = 248$$

$$(3.9) \quad \nu = \sqrt{\frac{1.2571}{1.257 - 1}} \tan^{-1} \sqrt{\frac{1.257 - 1}{1.257 + 1} (2.3^2 - 1)} - \tan^{-1} \sqrt{(2.3^2 - 1)} = 39.387$$

(3.10)

$$\theta_{max} = \frac{39.387}{2} = 19.694$$

(3.11)

$$K- = (19.694/10) + (19.694/10) = 3.939$$

(3.12)

$$K+ = 19.694/10 - 19.694/10 = 0$$

(3.13)

$$\theta = \frac{1}{2}[(3.939) + (0)] = 1.9694$$

(3.14)

$$\nu = \frac{1}{2}[(3.939) - (0)] = 1.9694$$

(3.15)

$$C- = \frac{1}{2}(1.9695 + 5.9081) - \frac{1}{2}(62.1340 + 50.8017) = -52.5290deg$$

(3.16)

$$C+ = \frac{1}{2}(3.9387 + 5.9081) + \frac{1}{2}(55.3704 + 50.8017) = 58.010 deg$$

(4.1)

$$T_{SYNODIC} = \frac{365.26 * 687.99}{|365.26 - 687.99|} = 778.65 days$$

(4.2)

$$T_{LAUNCH} = July\ 2020 + 1 * 778.65 = August\ 2020$$

(4.3)

$$\Delta V_{DEPARTURE} = \sqrt{\frac{1.327 \cdot 10^{20}}{1.496 \cdot 10^{11}}} \left(\sqrt{\frac{2 * 2.279 \cdot 10^{11}}{1.496 \cdot 10^{11} + 2.279 \cdot 10^{11}}} - 1 \right) = 2.94 \cdot m/s$$

(4.4)

$$\Delta V_{ARRIVAL} = \sqrt{\frac{1.327 \cdot 10^{20}}{1.496 \cdot 10^{11}}} \left(1 - \sqrt{\frac{2 * 2.279 \cdot 10^{11}}{1.496 \cdot 10^{11} + 2.279 \cdot 10^{11}}} \right) = 2.65 \cdot 10^3 m/s$$

(4.5)

$$T_{TRANSIT} = \frac{\pi}{\sqrt{1.327 \cdot 10^{20}}} \left(\frac{1.496 \cdot 10^{11} + 2.279 \cdot 10^{11}}{2} \right)^{3/2} = 258.8 \text{days}$$

(4.6)

$$T_{SURFACE} = \frac{-2 * \left(\pi - \frac{2\pi}{365.26} \frac{\pi}{\sqrt{1.327 \cdot 10^{20}}} \left(\frac{1.496 \cdot 10^{11} + 2.279 \cdot 10^{11}}{2} \right)^{3/2} \right) - 2\pi 1}{\frac{2\pi}{687.99} - \frac{2\pi}{365.26}} = 453.8 \text{days}$$